# Myopic Maculopathy

# 17

Yuxin Fang and Kyoko Ohno-Matsui

## 17.1 Introduction

The development of myopic macular lesions is characteristic to pathologic myopia (Figs. 17.1 and 17.2), and various lesions of myopic maculopathy have been well-known since a long time ago (see Chap. 1 for details). Thus, Schweizer (1890) examined 2910 myopes and found the changes at the macula in 6.3% of all myopes, in 14% of myopes above 3 diopters (D), and in 100% above 20D. Myopic macular complications described by Schweizer (1890) and later Sattler (1907) include macular hemorrhages, white spots of atrophy, and an atrophic sclerosis of the small vessels, although later studies have revealed that the choroidal vessels were not truly sclerotic. They also described that eventually large areas of atrophy may appear, until the choroid and retina may have disappeared over a wide area of the central region. A central circular dark spot (the Förster-Fuchs spot), which is now considered a proliferation of retinal pigment epithelium (RPE) around myopic choroidal neovascularization (CNV), was first clinically described by Forster (1862), first anatomically examined by Lehmus (1875), and extensively studied by Fuchs (1901). Lacquer cracks were found by Salzmann in 1902 as cleft-shaped or branched defects in the lamina vitrea (an ancient name for Bruch's membrane) [1, 2].

Curtin did outstanding observations of various kinds of lesions of myopic maculopathy [3]. He analyzed the development of myopic maculopathy in association with posterior staphyloma and also according to the patients' age (birth to age 30, ages 30 to 60, and age 60 or above). Grossniklaus and Green [4] performed histological analyses of the eyes with myopic maculopathy and provided important insights in understanding the pathologies of myopic maculopathy. Avila [5] graded myopic maculopathy on a scale of increasing severity.

Later Tokoro updated and organized the lesions of myopic maculopathy in his atlas [6]. Tokoro [6] classified myopic macular lesions into four kinds of categories based on ophthalmoscopic findings: (1) tessellated fundus (Fig. 17.2a), (2) diffuse chorioretinal atrophy (Fig. 17.2b), (3) patchy chorioretinal atrophy (Fig. 17.2c), and (4) macular hemorrhage (Fig. 17.2d). Macular hemorrhage was subclassified into two types of lesions—myopic CNV and simple macular hemorrhage. Later, Hayashi et al. [7] made some modifications and considered lacquer cracks as an independent lesion from diffuse atrophy (Table 17.1). Each of these lesions is explained in detail in this chapter.

Myopic maculopathy is important because it is often bilateral and irreversible, and it frequently affects individuals during their productive years. Because the definition of myopic maculopathy is different among studies, it is impossible to simply compare the results of different studies. However, myopic maculopathy is the leading cause (22%) of blindness in Japanese adults aged 40 years or older [8], the third cause (6.6%) of blindness in Chinese adults 50 years and older in urban southern China [9], and the third cause (6.7%) of visual impairment in the ethnic Indians aged more than 40 years living in Singapore [10]. A survey of 2263 Japanese adults aged 40–79 years showed that the OR of visual impairment for myopic adults was 2.9 (95% CI 1.4, 6.0) [11]. Besides East Asian countries, myopic maculopathy is currently the third cause of blindness in the adult Latinos aged 40 years or older in the USA [12], the second cause of bilateral blindness in an elderly urban Danish population [13], the fourth common cause of visual impairment in the elderly in UK [14], and the third most common cause of blindness in the working age population in Ireland [15] and Israel [16]. A recent study of

Y. Fang · K. Ohno-Matsui (✉)
Department of Ophthalmology and Visual Science, Tokyo Medical and Dental University, Bunkyo-Ku, Tokyo, Japan
e-mail: k.ohno.oph@tmd.ac.jp



R. F. Spaide et al. (eds.), *Pathologic Myopia*, https://doi.org/10.1007/978-3-030-74334-5_17

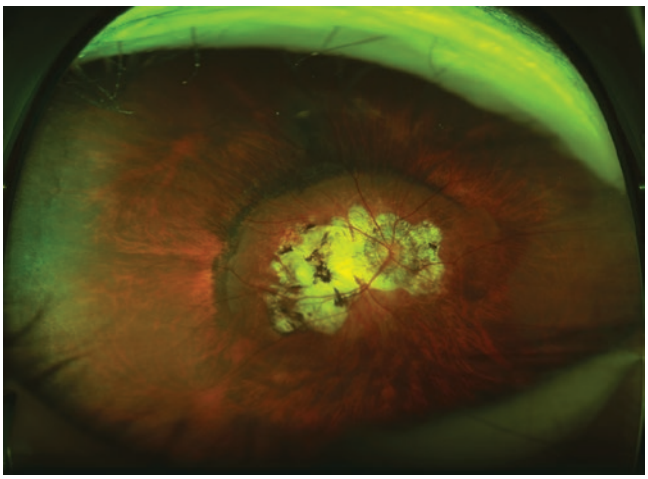

**Fig. 17.1** Ultra-wide fundus photograph of an eye with pathologic myopia. An extensive chorioretinal atrophy fused with a large myopic conus is seen within the area of posterior staphyloma

4582 Chinese-American adults aged 50+ years revealed that the most common cause of blindness was myopic retinopathy [17]. Actually, the visual prognosis for highly myopic patients with myopic maculopathy was poorer than for those without maculopathy [18]. Earlier population-based studies showed a correlation between worse corrected visual acuity and a presence of myopic maculopathy [19, 20].

Recent advance in ocular imaging, especially optical coherence tomography (OCT), has provided novel and important information in the interpretation of myopic maculopathy. Thus, in this chapter, we will overview the features of each lesion of myopic maculopathy with the latest knowledge obtained by the latest technologies.

## 17.2 Features of Each Lesion of Myopic Maculopathy

### 17.2.1 Tessellated (or Tigroid) Fundus

In eyes with high myopia, hypoplasia of the retinal pigment epithelium (RPE) following axial elongation reduces the pigment, allowing the choroidal vessels to be seen (Fig. 17.2a). Tessellated fundus is one of the earliest visible signs in eyes with high myopia, like the myopic conus around the optic disc. Tessellation begins to develop around the optic disc, especially in the area between the optic disc and the central fovea. Although it is rare to detect other myopic fundus lesions (e.g., myopic chorioretinal atrophy or CNV) in the children and young patients with high myopia [21], tessellated fundus is often observed in children with high myopia. Highly myopic patients with tessellated fundus are significantly younger than the patients with other lesions of myopic maculopathy [7, 22]. Wang et al. [22] reported that the highly myopic patients with tessellated fundus alone had less myopia, shorter axial length, and less staphyloma than the highly myopic patients with diffuse chorioretinal atrophy. Tokoro [6] reported that about 90% of eyes with only tessellated fundus and no chorioretinal atrophy had an axial length less than 26 mm. This percentage decreases linearly in eyes with longer axial length and becomes 0 when the axial length is longer than 31 mm. Actually, a 1-mm elongation in axial length will lead to about a 13% increase of chorioretinal atrophy from eyes with only tessellated fundus and no chorioretinal atrophy.

What causes the tessellation of the fundus is not clear. The RPE cells become thinned due to a stretching and expansion of the posterior globe in the studies using animal models of experimental myopia [23, 24]. Also, the earlier studies using vitreous fluorophotometry showed that retinal blood barrier was damaged in myopic subjects already under the age 40 [25] and also in animal models of experimental myopia [26–28]. Tessellation can also be seen in other conditions as well, e.g., the fundus of the elderly or in chronic stages of Vogt-Koyanagi-Harada disease (as sunset glow fundus). Spaide [29] analyzed the features of the patients with age-related choroidal atrophy (choroidal thickness was less than 125 ⌈m) and reported that all eyes had a tessellated fundus appearance. The mean (or median) choroidal thickness at subfovea in eyes with tessellated fundus in high myopia varies from 80 to 166 μm [22, 30–32], and choroidal thickness at all locations reduced almost by one-half compared to those with no myopic maculopathy in high myopia [30, 31]. These suggest that an attenuation of choroid occurs and RPE abnormalities could then develop.

Tessellation alone does not usually cause a decreased visual acuity, although it has been reported there are reduced amplitude and a delayed latency of multifocal ERG in highly myopic eyes with tessellated fundus alone [33–36].

In the study investigating the natural course of 806 eyes of 429 consecutive patients with high myopia (myopic refractive error >8 D or axial length ε 26.5 mm) for 5 to 32 years [7], only 13.4% of eyes with a tessellated fundus showed a progression; 10.1% developed diffuse chorioretinal atrophy, 2.9% developed lacquer cracks, and 0.4% developed a CNV. Progression was also observed in 19% in 10-year follow-up in Beijing Eye Study [37]. Another large series of 810 highly myopic eyes who followed more than 10 years (a mean follow-up of 18 years) showed 27% of eyes with tessellated fundus progressed in which 74.3% progressed to diffuse atrophy, 21.6% progressed to patchy atrophy, 10.8% developed new lacquer cracks, and 6.8% developed myopic CNV [38]. Since the eyes with other myopic fundus lesions showed a higher progression rate to the more advanced lesions than the eyes with tessellated

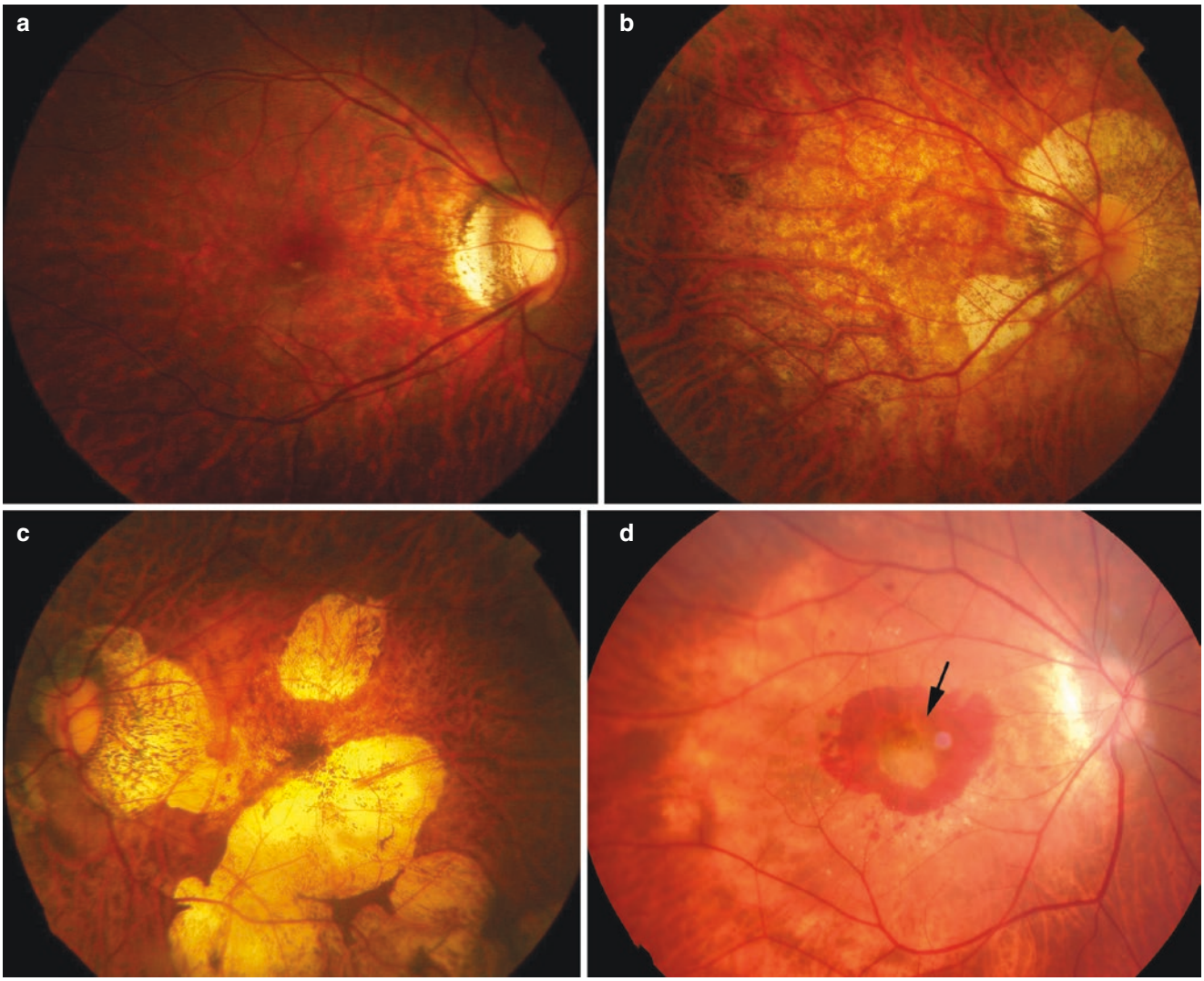


**Fig. 17.2** Fundus lesions according to a classification of myopic maculopathy by Tokoro in 1998. (**a**) Tessellated fundus. Large choroidal vessels can be seen in the posterior fundus as a relief. (**b**) Diffuse chorioretinal atrophy. Yellowish, ill-defined atrophy is seen in the posterior fundus. (**c**) Patchy chorioretinal atrophy. Multiple lesions of well-defined whitish atrophy (as white as myopic conus) exist within the area of diffuse atrophy. (**d**) Macular hemorrhage. The fibrovascular membrane suggesting choroidal neovascular membrane (arrow) is also noted in this case

**Table 17.1** Lesions of myopic maculopathy based on the natural progression (Hayashi et al. 2010)

| |
|---|
| Tessellated fundus |
| Diffuse chorioretinal atrophy |
| Lacquer cracks |
| Patchy chorioretinal atrophy |
| Myopic choroidal neovascularization |

fundus, it is suggested that myopic maculopathy tends to progress more quickly after the myopic maculopathy has advanced past the tessellated fundus stage. A tessellated fundus might be a relatively stable condition, and highly myopic eyes might stay in this condition for a relatively long period.

### 17.2.2 Lacquer Cracks

Lacquer cracks are fine, irregular, yellow lines, often branching and crisscrossing, seen in the posterior fundus of highly myopic eyes (Fig. 17.3). Stereoscopic observation using magnified lens (e.g., +90D or +75D lens) shows that lacquer cracks are somewhat depressed compared to the surrounding retina. Larger choroidal vessels frequently traverse the lesions posteriorly. In rare occasions, lacquer cracks are also observed in the mid-periphery [39] or nasal to the optic disc [40]. Pruett et al. [41] analyzed the pattern of break formation in eyes with lacquer cracks, angioid streaks, or traumatic tears in Bruch's membrane. Lacquer cracks were found in a reticular distribution within a posterior staphyloma; angioid

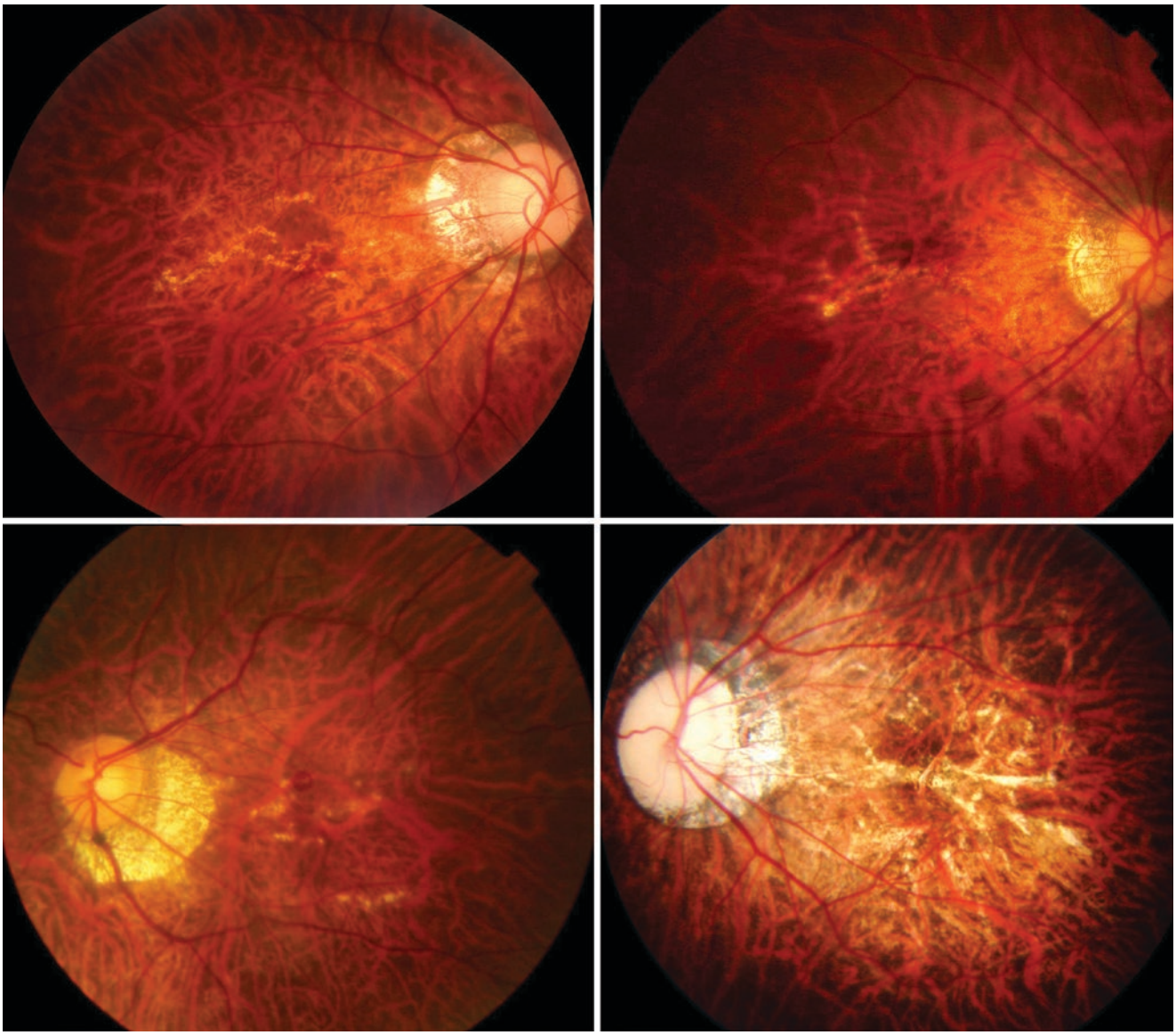

**Fig. 17.3** Lacquer cracks. Lacquer cracks are observed as yellowish linear lesions which run in parallel or in crisscross pattern. Large choroidal vessels are observed to course posteriorly

streaks occurred in a spider-web configuration centered on the optic nerve; traumatic tears were characteristically curved, perineural, and eccentric temporally. Curtin and Karlin [42] reported that lacquer cracks were found in 4.3% of highly myopic eyes. Histologically, the lacquer cracks represent healed mechanical fissures in the RPE-Bruch's membrane-choriocapillaris complex [4].

Lacquer cracks can develop at a relatively early age in highly myopic patients (e.g., in the 30s). The greatest incidence of lacquer cracks was noted in the age groups of 20 to 39 years. Klein and Curtin [43] reported that the mean age of the patients with lacquer cracks was 32 years with a range of 14 to 52 years. Tokoro [6] reported that the frequency of lacquer cracks was low in patients younger than age 20 and in the elderly but increases around ages 40 and 60 years. The frequency distribution of lacquer cracks showed two peaks in the age between 35 and 39 years and the age between 55 and 59 years.

The diagnosis of lacquer cracks has been mainly based on ophthalmoscopic identification. Fluorescein angiography (FA) has been an additional standard method to detect lacquer cracks [43]. Lacquer cracks show a consistent linear hyperfluorescence during the entire angiographic phase (Fig. 17.4), a window defect due to RPE atrophy overlying the defects of Bruch's membrane in the early angiographic phase and a staining of healed scar tissue filling the Bruch's membrane defect in the late phase. However, especially in the eyes with diffuse chorioretinal atrophy, it is sometimes

difficult to observe yellowish lacquer cracks within the area of yellowish diffuse atrophy and also difficult to detect linear hyperfluorescence of lacquer cracks within mildly stained diffuse atrophy. The usefulness of indocyanine green angiography (ICGA) has also been reported [44–49]. Lacquer cracks are observed as linear hypofluorescence during the entire angiographic phase of ICGA. The hypofluorescence in ICGA is more easily recognized in late angiographic phase, because an intense fluorescence of retrobulbar blood vessels or large choroidal vessels impairs the observation of narrow linear hypofluorescence of lacquer cracks in the early angiographic phase. In some cases, lacquer cracks observed by ICGA are more numerous and longer than those observed by FA. Also, ICGA can detect the lacquer cracks even at the onset of rupture of Bruch's membrane as linear hypofluorescence beneath the subretinal bleeding [46]. Lacquer cracks also show linear hypo-autofluorescence by fundus autofluorescence (Fig. 17.4). It is difficult to detect lacquer cracks by using OCT, because it is such a narrow lesion. However, in some cases, the discontinuities of the RPE (and probably Bruch's membrane as well) and an increased penetrance into the deeper tissue beyond the RPE are observed at the site of the lacquer cracks (Fig. 17.4). Once detected, OCT is considered to be the most accurate diagnostic tool, because only OCT can visualize the discontinuity of Bruch's membrane, which is an integral feature of lacquer cracks.

When the mechanical rupture of Bruch's membrane occurs, subretinal macular hemorrhage without CNV develops (Fig. 17.5) [50–52]. This subretinal bleeding is absorbed spontaneously, and after absorption we can observe lacquer cracks as yellowish linear lesion at the corresponding area of previous bleeding. Most of the patients with subretinal bleeding without CNV have a good visual recovery after absorption of hemorrhage. However, in the eyes whose bleeding was thick and penetrated into the inner retina beyond the external limiting membrane, the IS/OS defect seen at the onset by using OCT remains after absorption of hemorrhage, leaving the permanent vision loss [53].

Lacquer cracks might be a unique lesion among the various lesions of myopic maculopathy, because they seem to be caused almost purely by mechanical expansion of the globe and are not much influenced by aging. This is supported by the fact that chick models of experimental myopia which can

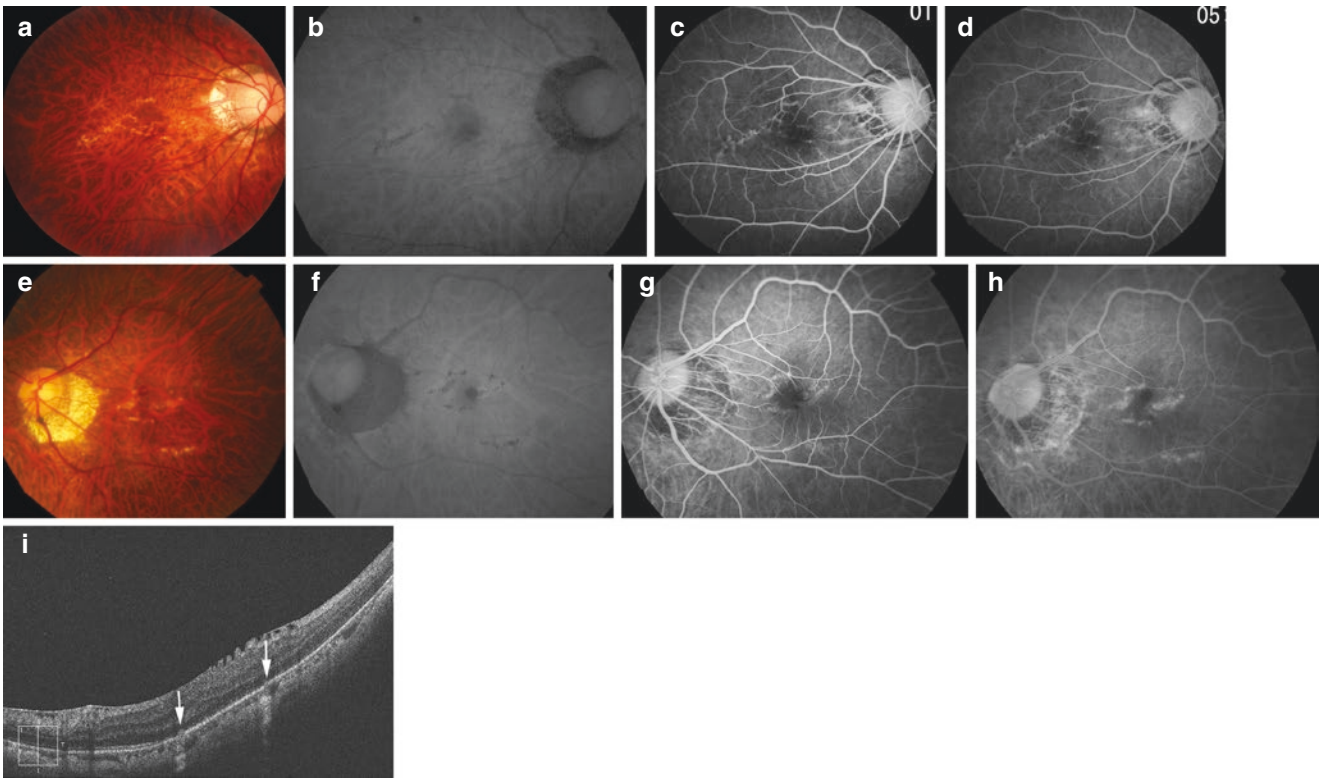


**Fig. 17.4** Angiographic and optical coherence tomographic (OCT) findings of lacquer cracks. (**a**) Right fundus shows multiple lacquer cracks as fine, irregular, yellow lines, branching and crisscrossing in the posterior fundus. Larger choroidal vessels frequently traverse the lesions posteriorly. (**b**) Fundus autofluorescence (FAF) shows lacquer cracks as linear hypo-autofluorescence. (**c**, **d**) Fluorescein angiographic (FA) findings. Lacquer cracks show linear hyperfluorescence from the early angiographic phase (**c**) to the late phase (**d**). (**e**) Left fundus shows multiple lacquer cracks which run in parallel. (**f**) FAF shows linear hypo-autofluorescence corresponding to lacquer cracks. (**g**, **h**) Lacquer cracks show linear hyperfluorescence from the early angiographic phase (**g**) to the late phase (**h**) by FA. (**i**) OCT findings show the discontinuities of retinal pigment epithelium and deep penetrance of the light signal at the corresponding site of lacquer cracks

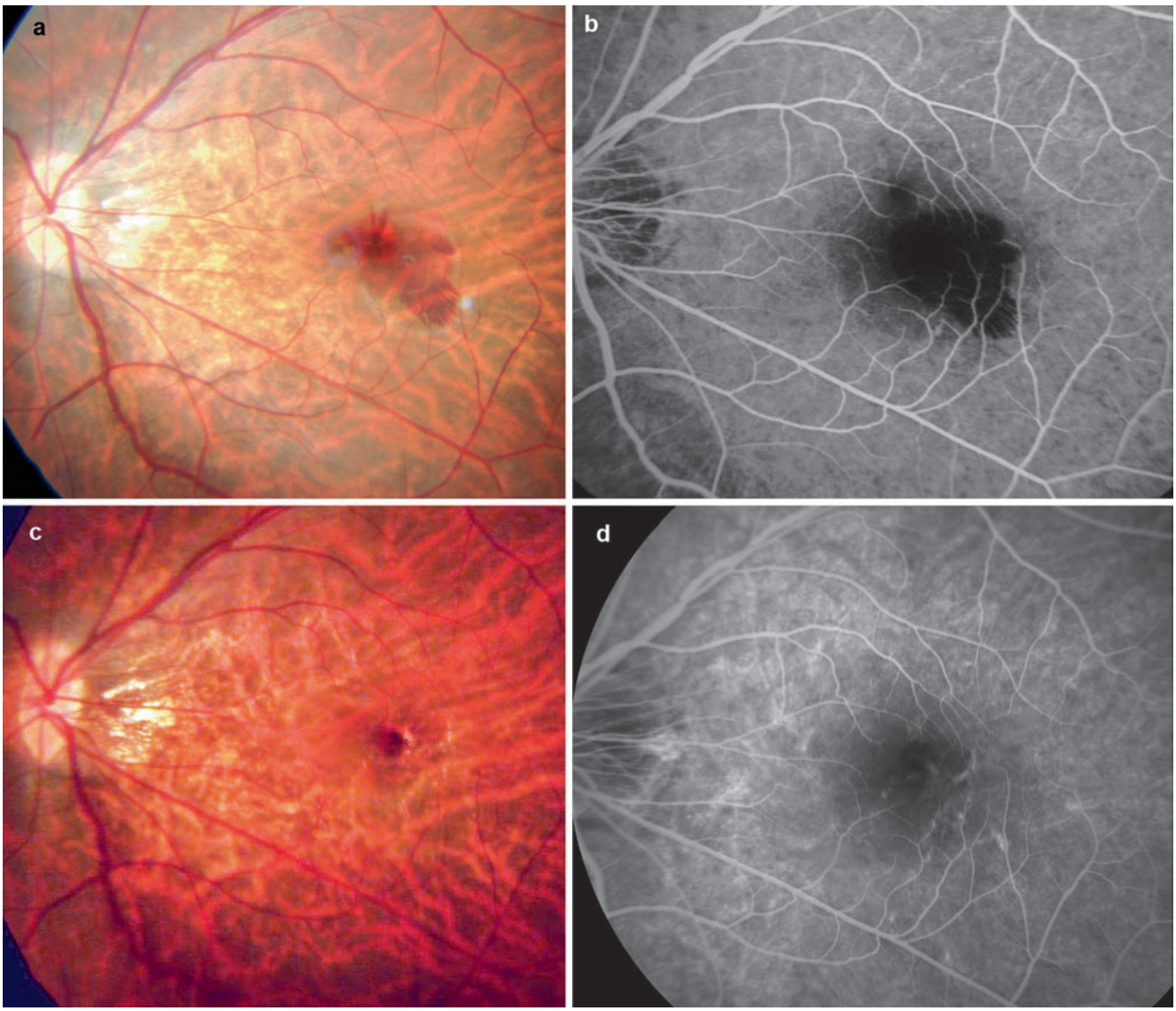


**Fig. 17.5** Subretinal bleeding without choroidal neovascularization as a sign of new lacquer crack formation. (**a**) Left fundus shows subretinal bleeding in the macula. (**b**) Fluorescein angiogram (FA) shows a blocked fluorescence due to bleeding. (**c**) Two months later, the bleeding is absorbed spontaneously. Lacquer cracks are observed at the site of the previous bleeding. (**d**) FA shows lacquer cracks as linear hyperfluorescence

develop axial myopia in 2 weeks of visual deprivation can develop lacquer cracks [54]. Actually, lacquer cracks and subretinal bleeding caused by a new lacquer crack formation have been the only macular pathologies which reportedly develop in animal models of experimental myopia. This is also supported that lacquer cracks develop after LASIK surgery [55–59] or after laser photocoagulation [60].

Once lacquer cracks develop in the eye, it tends to develop one after another in the same eye. Thus, the patients with lacquer cracks tend to have multiple lacquer cracks in both eyes. It seems that there might be a genetic predisposition toward lacquer crack formation among individuals with pathologic myopia.

There is no obvious correlation between the axial length and lacquer cracks in eyes with pathologic myopia. Klein and Curtin [43] reported that the mean axial length of the eyes with lacquer cracks was 31.8 mm (range, 29.8–34.7 mm). Tokoro [6] reported that the largest number of eyes with lacquer cracks appears between 29.0 and 29.4 mm.

It is uncommon for lacquer cracks to develop across the central fovea. Thus, lacquer cracks themselves do not usually impair the central vision; however, the subretinal bleeding

which develops at the onset of the rupture of Bruch's membrane could cause the impairment of central vision even after absorption of the hemorrhage.

The Blue Mountains Eye Study (BMES) reported that 8.7% had new or increased numbers of lacquer cracks in 5 years [61]. In the follow-up study of 66 eyes with lacquer cracks for an average of 72.8 months (range, 7 to 243 months) [62], lacquer cracks progressed in 37 eyes (56.1%). Of these 37 eyes, the number of lacquer cracks increased in 14 eyes and turned into other myopic fundus changes in 25 eyes. These changes included patchy atrophy, diffuse atrophy, and CNV. In another study [7], 75 eyes with lacquer cracks were followed for more than 5 years and found that 32 eyes (42.7%) showed an increase in the width of the cracks and these eyes progressed to patchy chorioretinal atrophy (Fig. 17.6), 10 eyes (13.3%) developed CNV, and 10 eyes (13.3%) had an increase in number of lacquer cracks. The patchy atrophy that progressed from lacquer cracks is usually longitudinally oriented oval or rectangular (Fig. 17.6). The progression toward the patchy atrophy from lacquer cracks represents an increased area of rupture of Bruch's membrane. Thus, this progression is an increased area of macular Bruch's membrane defect (or opening). Xu [63] showed that the progression from lacquer cracks to patchy atrophy was not a uniform widening of the preexisting lacquer cracks but small circular areas of patchy atrophy that developed first along the lines of lacquer cracks, and then these circular areas enlarged and fused with each other. So, perhaps when the Bruch's membrane ruptures, the overlying RPE may remain continuous because the Bruch's membrane rupture is narrow. Later with increasing mechanical tension, the overlying RPE ruptures, and RPE hole develops. This suggests that the RPE-Bruch's membrane complex does not disrupt simultaneously during lacquer crack formation.

Although lacquer cracks are often observed in the vicinity of CNV [5], it is unexpectedly uncommon for CNV to develop from the existing lacquer cracks. This suggests that the lacquer cracks which are observed as yellowish linear lesions are already-healed scar tissue and CNV could rarely develop once after the Bruch's rupture is healed completely by the scar tissue. When CNV develops in relation to lacquer cracks, new vessels might penetrate through Bruch's membrane defects just after the rupture occurs and before the rupture is sealed by the scar tissue. Cases which develop CNV shortly after the subretinal bleeding without CNV support this hypothesis.

**Differential Diagnosis** Myopic stretch lines

Myopic stretch lines were first reported by Dr. Yannuzzi [64] as hyper-autofluorescent linear lesions in the posterior fundus of highly myopic eyes (Fig. 17.7). Myopic stretch lines are observed as pigmented, brown lines alongside the large choroidal vessels (Fig. 17.7); however, it is sometimes difficult to observe this lesion funduscopically, and in that case only FA provides a clue of this lesion. Myopic stretch lines almost always develop in eyes with severe diffuse atrophy with a posterior staphyloma. Although ICGA showed similar findings (linear hypofluorescence) in two types of linear lesions in the posterior fundus of highly myopic eyes

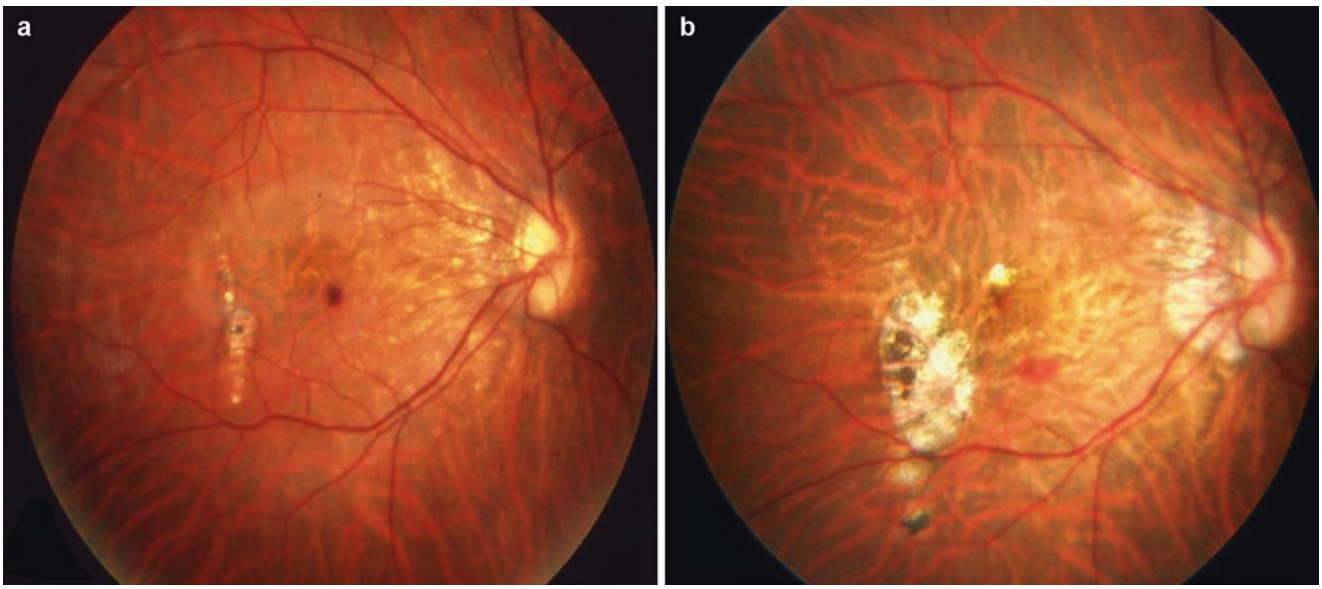


**Fig. 17.6** Progression to patchy chorioretinal atrophy from lacquer cracks. (**a**) Right fundus of a 28-year-old woman shows a lacquer crack temporal to the central fovea. (**b**) Five years later, the width of the lacquer crack increased and progressed to patchy atrophy. New lacquer cracks are formed upper and lower to the fovea, and subretinal bleeding related to new lacquer crack formation is observed lower to the fovea

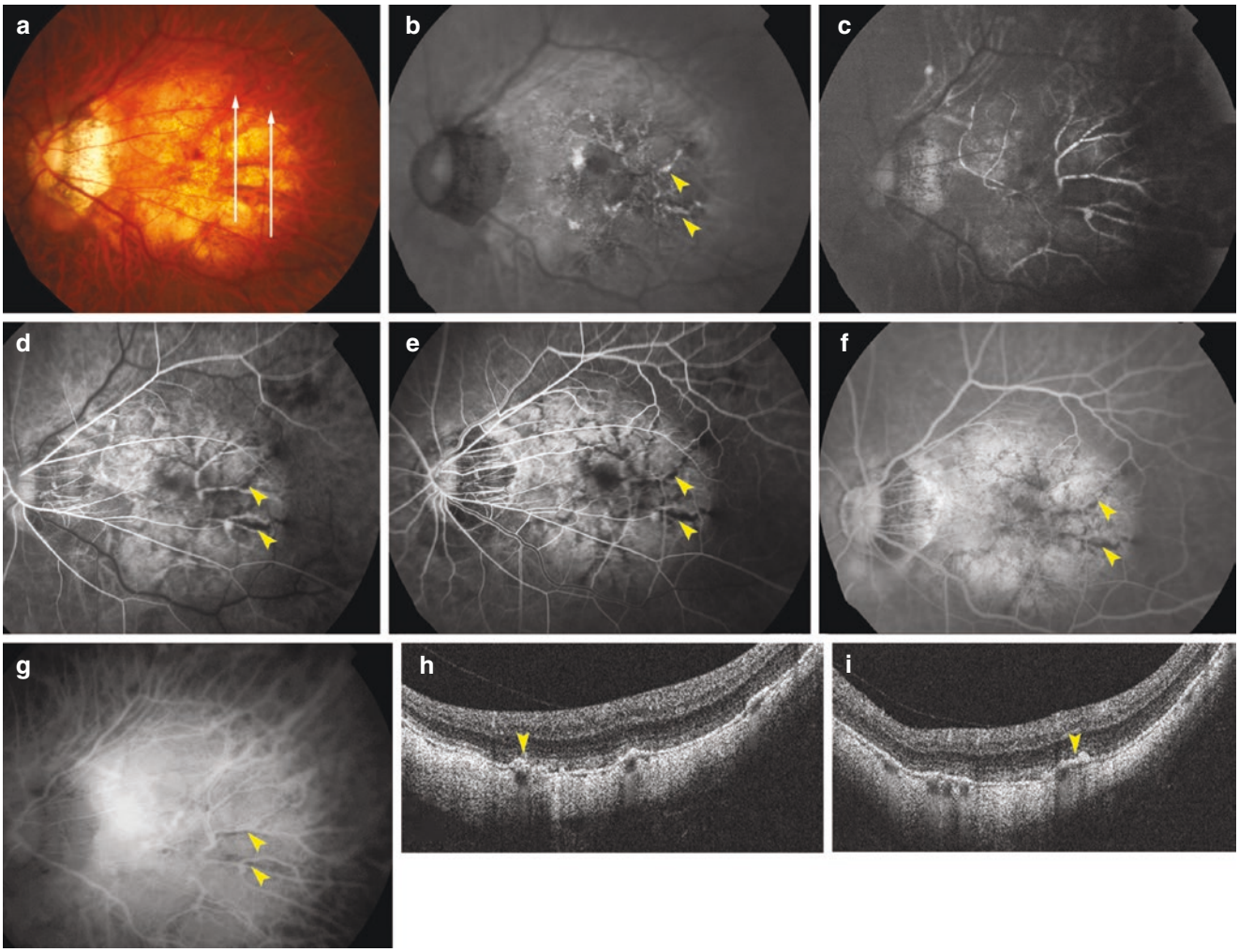


**Fig. 17.7** Myopic stretch lines. (**a**) Left fundus shows brownish, pigmented lines along the large choroidal vessels temporal to the macula. White lines show the scanned lines by OCT in (**h**) and (**i**). (**b**) Fundus autofluorescence (FAF) shows multiple lines with hyper-autofluorescence radiated around the central fovea. Arrowheads show the same point of the stretch lines between (**b**), (**d**), (**e**), and (**f**). (**c**) Choroidal phase of fluorescein angiography (FA) shows large choroidal arteries. Some parts of large choroidal arteries show hypofluorescent spots by blocked fluorescence of overlying stretch lines. (**d**) Retinal arterial phase of FA. Myopic stretch lines appear as hypofluorescent linear lesions. (**e**) Retinal venous laminar flow phase of FA. Myopic stretch lines are clearly observed as multiple hypofluorescent lines around the central fovea and within the slightly stained diffuse atrophy. (**f**) Late phase of FA clearly shows myopic stretch lines as multiple hypofluorescent lines within the slightly stained diffuse atrophy. (**g**) Late phase of indocyanine green angiography shows a mild hypofluorescence corresponding to the stretch lines. (**h**, **i**) OCT shows that the almost entire thickness of the choroid is absent and only large choroidal vessels are sporadically present. Large choroidal vessels seem to protrude toward the vitreous, and clumps and proliferation of retinal pigmented epithelium are seen on and around the choroidal vessels (arrowheads)

(lacquer cracks and myopic stretch lines), the features obtained funduscopically, angiographically, and by OCT were different between these two types of linear lesions. Contrary to lacquer cracks, fundus autofluorescence (FAF) showed linear hyper-autofluorescence in myopic stretch lines (Fig. 17.7). OCT images show the clumps of RPE or RPE proliferation on and around the large choroidal vessels (which are protruded toward the vitreous subsequent to a disappearance of most of the choroidal layers) (Fig. 17.7). These suggest that myopic stretch lines might represent the RPE proliferation on and around the remaining large choroidal vessels [65]. Because ICGA findings of myopic stretch lines are same with those of lacquer cracks and the diagnosis of lacquer cracks are sometimes based solely on ICGA in many studies, a caution is necessary for differentiating myopic stretch lines from lacquer cracks.

### 17.2.3 Diffuse Choroidal Atrophy

Diffuse choroidal atrophy is observed as ill-defined yellowish lesion in the posterior fundus of highly myopic eyes

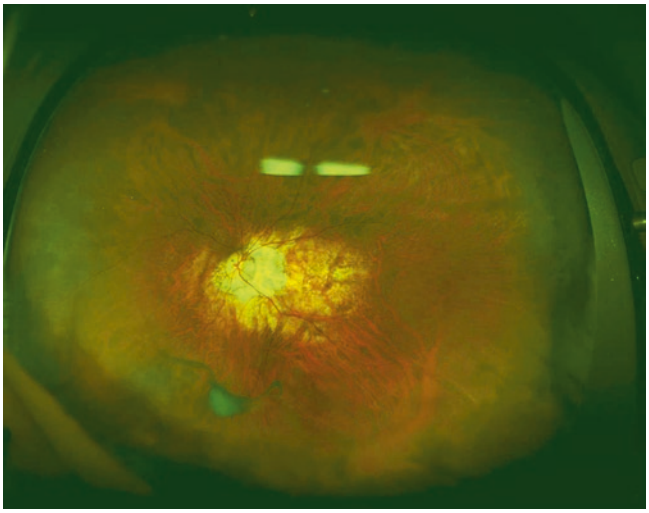

**Fig. 17.8** Ultra-wide fundus photograph of diffuse choroidal atrophy. A yellowish, ill-defined lesion is seen in the posterior fundus

(Figs. 17.8 and 17.9). This lesion begins to appear around the optic disc and increases with age and finally covers the entire area within the staphyloma (Fig. 17.9). When diffuse atrophy is observed only around the optic disc, it needs to be differentiated from peripapillary intrachoroidal cavitation (peripapillary ICC) [66–70], because ICC also shows similar ophthalmoscopic appearance regardless of the difference in OCT images (see Chap. 9 for ICC).

The frequency of diffuse atrophy increases with aging as well as an increased axial length [6]. Diffuse atrophy begins to appear in the posterior fundus at around the age 40 and is observed in about 30–40% after age 40 [6]. The increasing rate of diffuse atrophy is about 10.5% per 10 years [6]. When the axial length is within the range of 27 to 33 mm, the increase in the percentage of eye with diffuse atrophy can be calculated using a simple regression equation. The increased percentage is 13.3%/mm in the total number of myopic eyes, 9.4%/mm in eyes under age 40, and 12.2%/mm in eyes over age 40 [6].

FA shows the mild hyperfluorescence due to tissue staining in the late angiographic phase (Fig. 17.10). On ICGA, diffuse atrophy itself does not show clear abnormalities; however, a marked decrease of the choroidal capillary, the medium- and large-sized choroidal vessels, is seen in the area of diffuse atrophy, and the blood vessels in the back of the eye are sometimes seen through the sclera in the posterior pole (Fig. 17.10). Because the penetrating site of short posterior ciliary arteries moves to the edge of posterior staphyloma, the choroidal blood vessels in the posterior pole become less dense (Fig. 17.10). In accordance with a marked decrease of choroidal vessels by ICGA, OCT shows a marked thinning of the choroid in the area of diffuse atrophy (Fig. 17.10). In most of the cases, the choroid is almost absent except sporadically present large choroidal vessels (Fig. 17.10). The remaining large choroidal vessels appear to protrude toward the vitreous. It is interesting to know, even in the area where most of the choroidal layer is absent, the RPE layer and outer retina are present in the eyes with diffuse atrophy (Fig. 17.10). A presence of outer retina and RPE even in the area where most of the choroid is gone might explain a relatively preserved vision in eyes with diffuse atrophy. Okisaka [71] reported that the choroidal changes in pathologic myopia began from the obliteration of precapillary arterioles or postcapillary venules, then followed by an occlusion of choriocapillaris. Finally, large choroidal vessels are also obliterated, and the choroid seems to be absent. In parallel to the vascular changes in the choroid, choroidal melanocytes disappear as well. Although a choroid becomes thinned in eyes with tessellated fundus, the degree of choroidal thinning is much more serious in eyes with diffuse atrophy. And such disproportionate thinning of choroid compared to the surrounding tissue (RPE, outer retina, and sclera) might be a key phenomenon in diffuse atrophy.

Why diffuse atrophy shows yellow color is not clear. Diffuse atrophy is not uniformly yellow but shows granular yellow appearance (Fig. 17.10).

### 17.2.4 Patchy Chorioretinal Atrophy

Patchy chorioretinal atrophy is observed as a grayish-white, well-defined atrophy (Figs. 17.11 and 17.12) [6]. Due to an absence of RPE and most of the choroid, the sclera can be observed through transparent retinal tissue, which is considered to show white color. This lesion is also referred to as focal chorioretinal atrophy [3]. Large choroidal vessels seem to course within the area of patchy atrophy. In some cases, retrobulbar blood vessels are observed through the patchy atrophy with moving according to the gaze shift. Stereoscopic fundus examination shows that the area of patchy atrophy is somewhat excavated compared to surrounding diffuse atrophy. Pigment clumping is observed within the area of patchy atrophy especially along the margin of the atrophy or along the large choroidal vessels. FA as well as ICGA shows a choroidal filling defect in the area of patchy atrophy (Fig. 17.11), suggesting that this lesion is a complete closure of choriocapillaris [6].

Due to a subsequent loss of RPE in the area of patchy atrophy, the lesion shows a lack of fundus autofluorescence (Fig. 17.11). Using OCT, patchy atrophy is observed as a loss of most of the thickness of choroid, RPE, and outer retina (Fig. 17.11). Thus, the inner retina is directly on the sclera within the area of patchy atrophy. Swept-source OCT also showed the discontinuities of Bruch's membrane in the area of patchy atrophy [72, 73]. The RPE stopped outside of the margin of the macular Bruch's membrane defect. The edges of the macular Bruch's membrane defects showed an

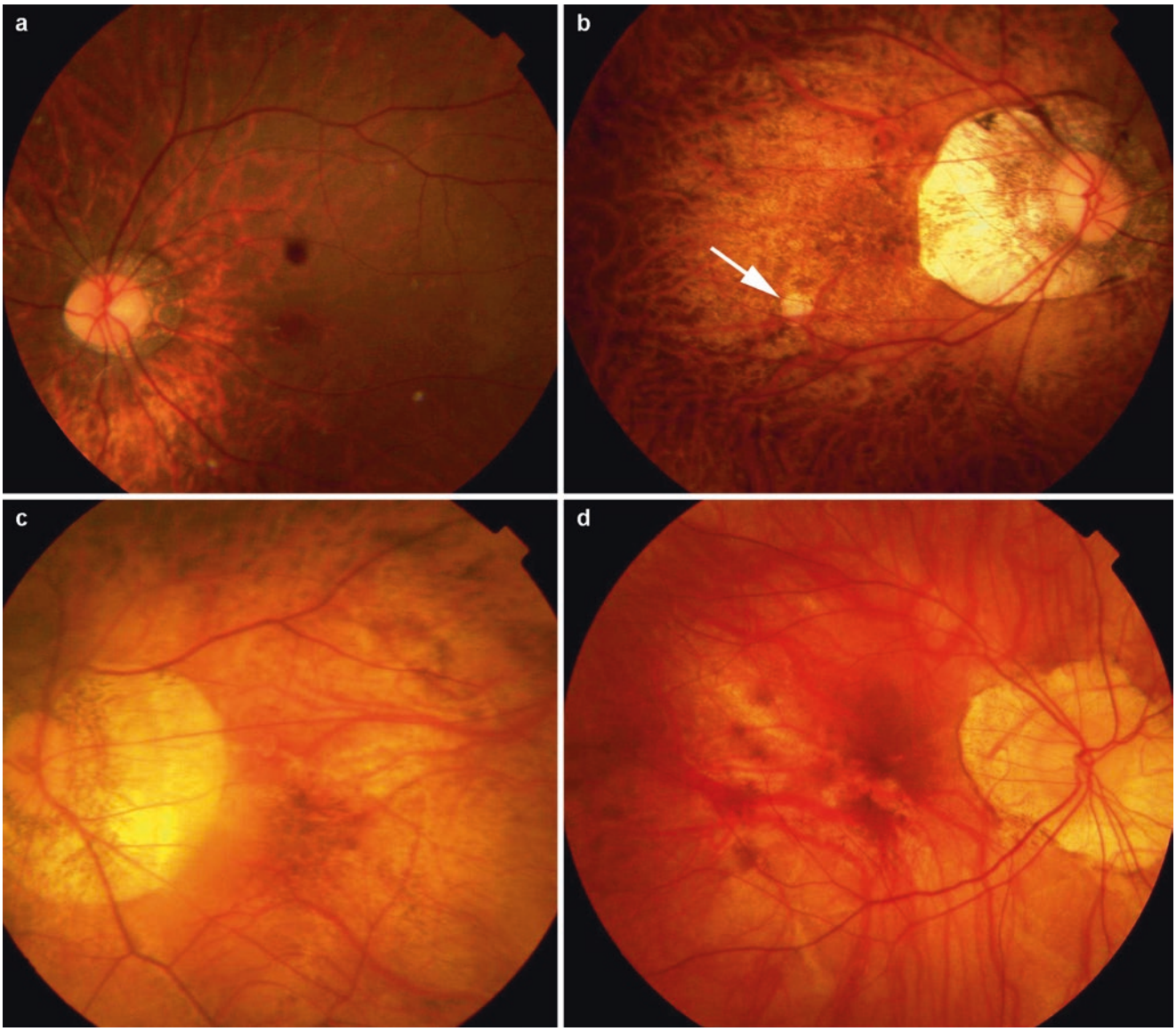


**Fig. 17.9** Diffuse choroidal atrophy. (**a**) Early stage of diffuse atrophy. Yellowish, ill-defined lesions are observed lower to the optic disc. (**b**) Advanced stage of diffuse atrophy. Yellowish, ill-defined atrophy covers the entire macular area. A small lesion of patchy chorioretinal atrophy (arrow) is also seen within the area of diffuse atrophy. (**c**) Advanced stage of diffuse atrophy. The posterior fundus within a staphyloma is replaced by diffuse atrophy. The images in (**a**) to (**d**) are Asians' eyes. (**d**) Diffuse atrophy in a Caucasian patient. Diffuse atrophy is seen evident especially in the lower fundus. Diffuse atrophy tends to be more obvious in the pigmented eyes

abrupt termination and often an upturned edge. This is contrary to the fact that the RPE, Bruch's membrane, and outer retina are preserved in most of the eyes with diffuse atrophy, although it is not certain if the remaining photoreceptors and RPE function normally in those eyes.

Patchy atrophy is subclassified into three types (Fig. 17.12): patchy atrophy which develops from lacquer cracks, P(Lc); patchy atrophy which develops within the area of an advanced diffuse chorioretinal atrophy, P(D); and patchy atrophy which can be seen along the border of the posterior staphyloma, P(St) [7]. P(D) is often circular or elliptical, and P(Lc) is longitudinally oval in its shape. P(Lc) is considered an enlargement of Bruch's membrane defect due to lacquer cracks, and P(D) might also represent a Bruch's membrane hole [74] developing within the area of advanced stage of diffuse atrophy. Jonas [74] recently reported that macular Bruch's membrane defects were found in 30.8% of highly myopic eyes whose axial length was ε 26.5 mm histologically. A lack of Bruch's membrane defects might be related to the development of macular ICC. Due to a lack of tensile Bruch's membrane in addition to a lack of choroid on the thin sclera, the area of patchy atrophy is very fragile against the inner pressure load. The sclera can be bowed posteriorly in the area of the patchy atrophy

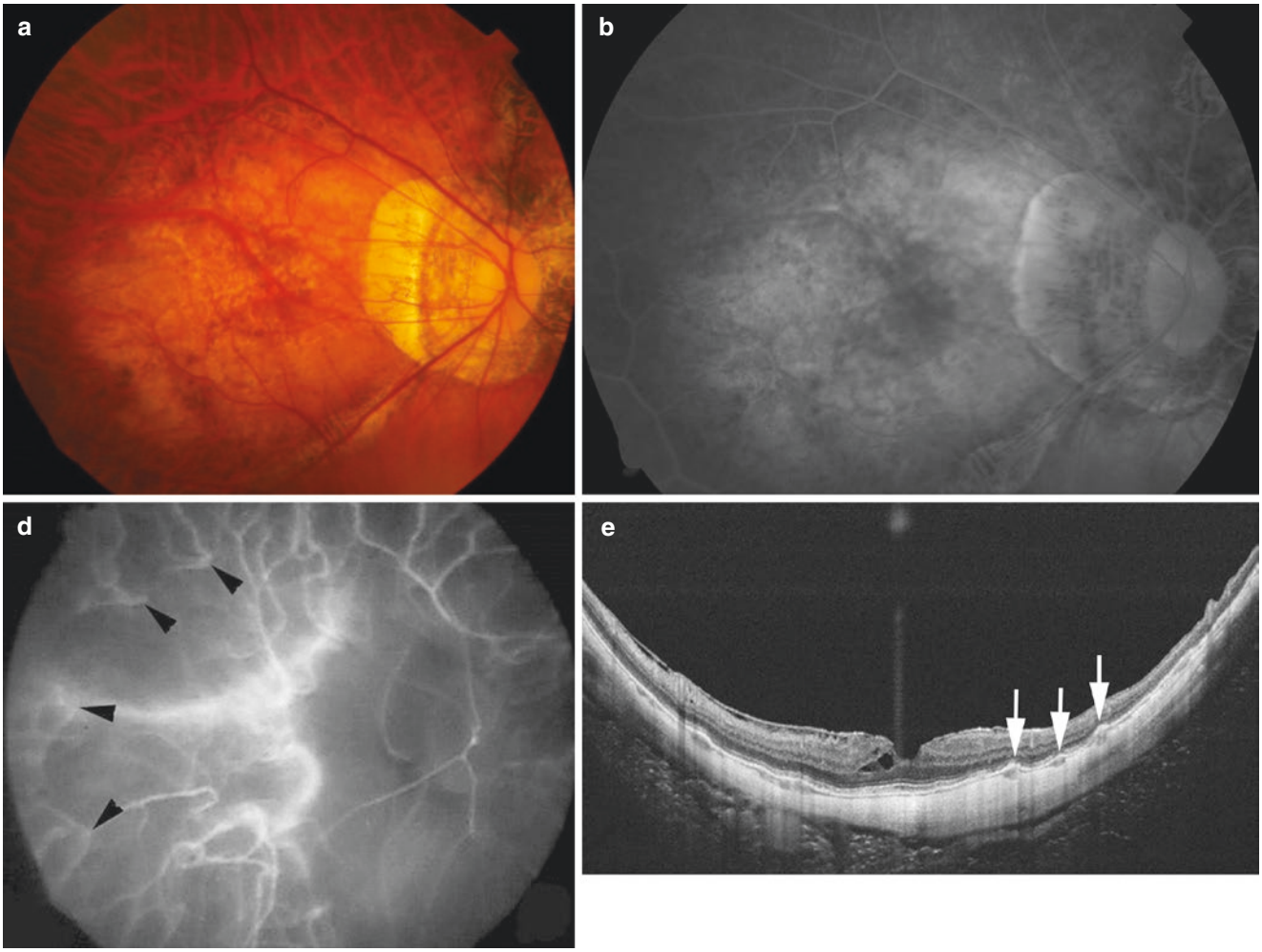


**Fig. 17.10** Angiographic and optical coherence tomographic (OCT) findings of diffuse choroidal atrophy. (**a**) Left fundus shows the diffuse choroidal atrophy in the posterior fundus. (**b**) Late angiographic phase of fluorescein angiogram shows slight hyperfluorescence in the area of diffuse atrophy. (**c**) Indocyanine green angiography shows that the penetrating site of short posterior ciliary arteries into the choroid is shifted toward the edge of posterior staphyloma. There are few large- and medium-sized choroidal vessels in the macular area, and instead retrobulbar blood vessels show an intense fluorescence. (**d**) OCT examination shows that most of the choroidal thickness is absent and only large choroidal vessels are sporadically present. Large choroidal vessels are observed to protrude toward the retina (arrows)

(Fig. 17.14), which resembles the intrachoroidal cavitation that develops adjacent to a myopic conus in highly myopic eyes (peripapillary intrachoroidal cavitations; peripapillary ICC). Thus, the posterior displacement of sclera can be called as macular ICC [75]. Macular retinoschisis is significantly more frequently observed in the eyes with macular ICC than those without macular ICC [75]. This is because the mechanical dissociation attributable to the scleral bowing and the caving in of the retina might facilitate the development of retinoschisis in and around the patchy atrophy.

Patchy atrophy is reportedly present in 0.4% of general population aged ≥ 40 years in the Hisayama Study in Japan [76]. The percentage of patchy atrophy increases linearly with axial length of the eye and reaches 32.5% after age 60 years [6]. The percentage of patchy atrophy is 3.3% in the eyes whose axial length is from 27 to 27.9 mm, which exceeds 25% if the axial length is longer than 31 mm, and it exceeds 50% if the axial length is longer than 32 mm [6].

With increasing age, the patchy atrophy enlarges and coalesces with each other [3, 7, 38]. In the follow-up study of 74 eyes with patchy atrophy for ε 5 years, 52 eyes (70.3%) showed a progression [7]. Fifty eyes (67.6%) showed an enlargement of the patchy areas, ten eyes (13.5%) showed a fusion with P(D) or P(St), and two eyes (2.7%) developed a CNV [7]. In the eyes with advanced enlargement and fusion of patchy atrophy, the posterior fundus shows a "bare sclera" appearance (Fig. 17.13). Almost all eyes (95%) with patchy atrophy progressed after a mean follow-up of 18 years, in which an enlargement of the original patchy atrophy was found predominantly in 98% and new patchy atrophy was found in 47% followed by development of myopic CNV in 21.7% and patchy-related macular atrophy in 8.3% [38].

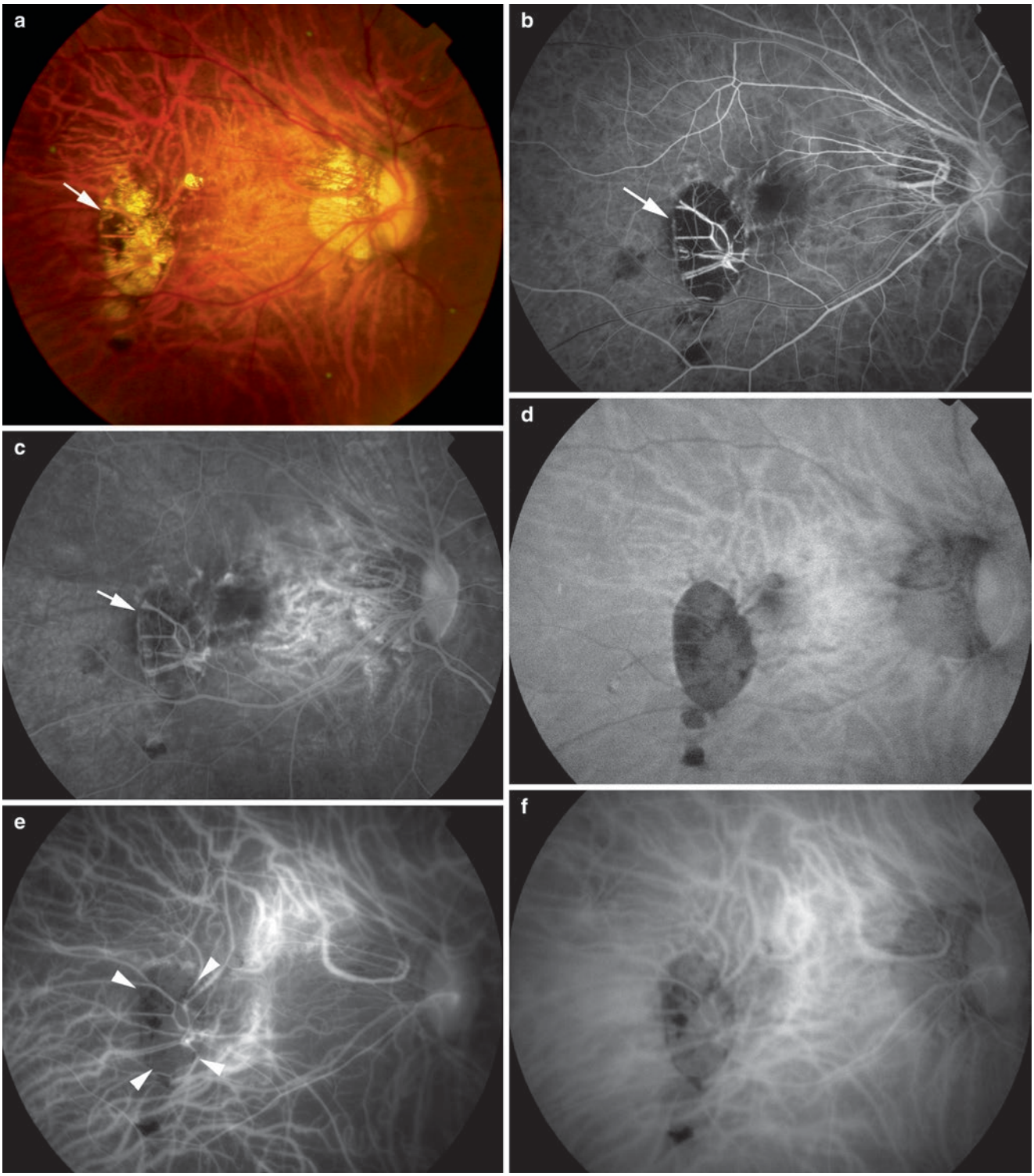


**Fig. 17.11** Patchy chorioretinal atrophy. (**a**) Right fundus shows a patchy atrophy (arrow) temporal to the central fovea. According to the subclassification of patchy atrophy, this case has P(Lc). (**b**) Early phase of fluorescein angiogram (FA) shows a hypofluorescence due to the choroidal filling defects (arrow). (**c**) In the late phase of FA, the margin of the lesion becomes slightly hyperfluorescent (arrow). (**d**) Fundus autofluorescence shows a distinct hypo-autofluorescence corresponding to the patchy atrophy. (**e**, **f**) Indocyanine green angiogram shows hypofluorescence due to choroidal filling defect from early angiographic phase (**e**; arrowheads) to late phase (**f**). (**g**) Optical coherence tomography examinations show that in addition to the absence of the entire thickness of the choroid, the retinal pigment epithelium as well as outer retina is absent (between arrowheads). The hyper-reflectivity in deep tissue due to an increased light penetration is noted in the area of patchy atrophy

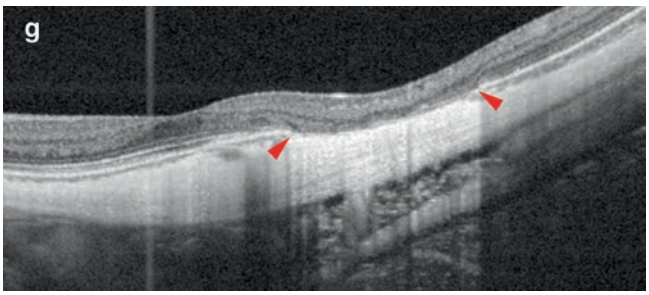


**Fig. 18.11** (continued)

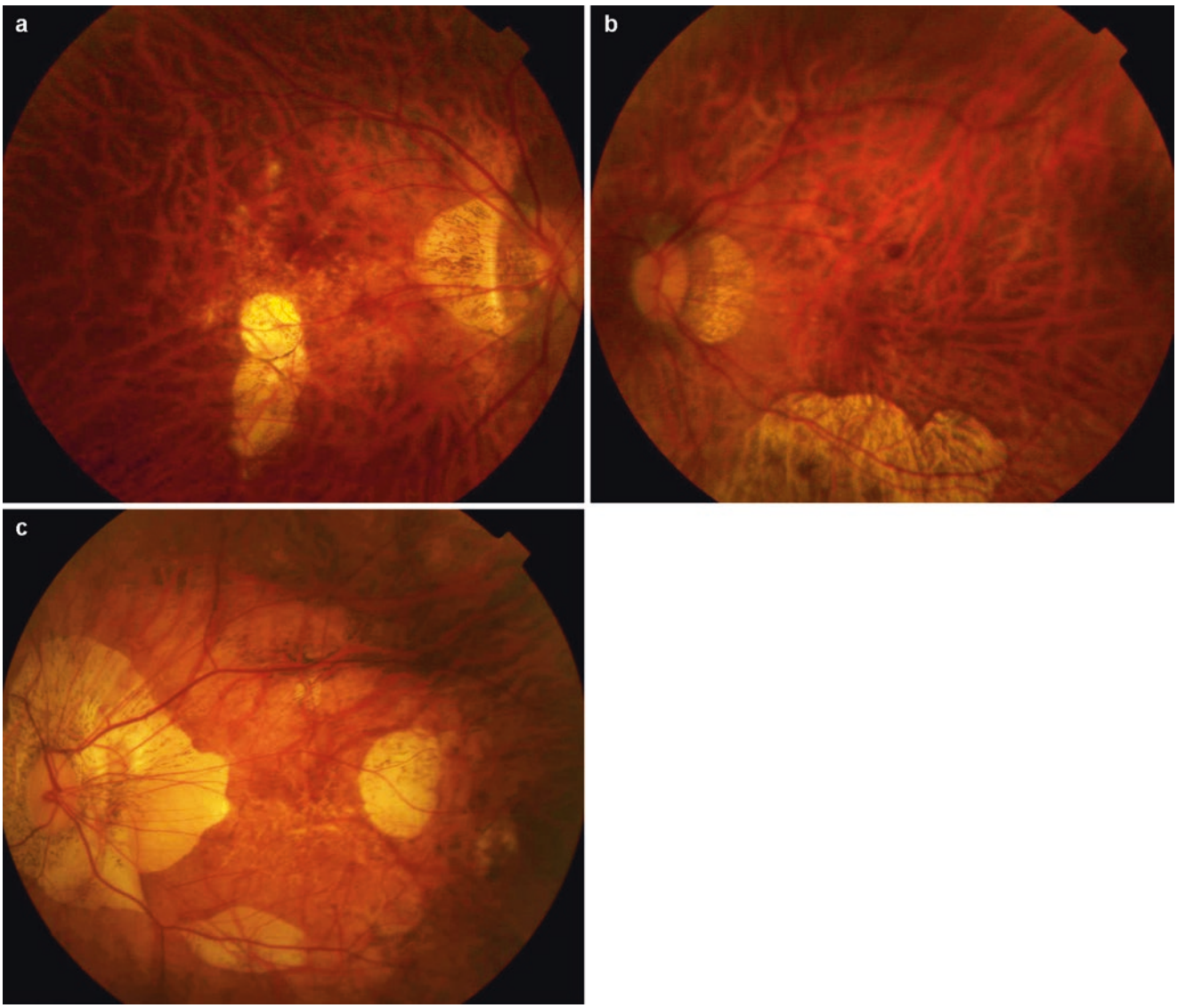


**Fig. 17.12** Three types of patchy chorioretinal atrophy. (**a**) P(Lc), patchy atrophy progressed from lacquer cracks. Longitudinal atrophy is seen lower to the central fovea. Lacquer cracks are also found in and around the central fovea, and the degree of background diffuse atrophy is mild. (**b**) P(St), patchy atrophy which develops along the edge of posterior staphyloma. (**c**) P(D), patchy atrophy which develops within the advanced stage of diffuse atrophy. An oval atrophy is observed temporal to the fovea. P(St) is also found along the lower edge of staphyloma

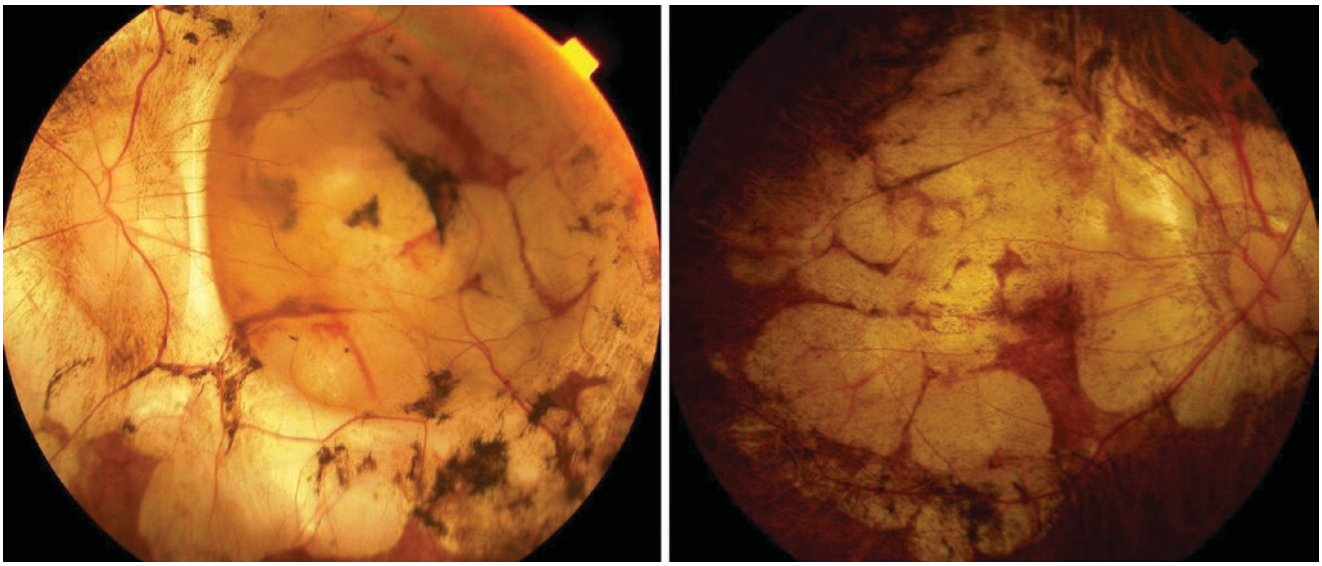

**Fig. 17.13** "Bare sclera" appearance due to an enlargement of patchy chorioretinal atrophy. The entire area of posterior fundus is replaced by an enlarged patchy atrophy

Such high percentages of progression of eyes with patchy atrophy could be explained by the biomechanical properties of Bruch's membrane so that as soon as a defect is created, the Bruch's membrane defect would enlarge over time with ongoing axial elongation. The BMES showed that 5.2% of the participants had new or expanded areas of patchy chorioretinal atrophy in 5 years [61]. Ito-Ohara et al. [77] examined the direction of enlargement of patchy atrophy and found that the patchy atrophy in marginal lesions of a staphyloma enlarged toward the macula and the patchy atrophy in the macula enlarged in all directions [77]. However, it is uncommon for extrafoveal patchy atrophy later to involve the central fovea. This means that it is rare for patchy atrophy to cause the central vision loss although this lesion causes a paracentral absolute scotoma due to a loss of photoreceptors within the atrophic area.

Various kinds of vitreoretinal complications can develop in and around the patchy atrophy. Probably due to a weak adhesion between the inner retina and sclera in the area of patchy atrophy, the macular retinoschisis tends to occur preferably in the area of patchy atrophy [78]. In the area of extensive chorioretinal atrophy, the diagnosis of retinoschisis needs caution because the retinoschisis shows less column-like structures [79]. It is also reported that posterior paravascular linear retinal breaks occur over areas of patchy atrophy as a cause of retinal detachment in the patients with pathologic myopia [80].

Although the patchy atrophy itself does not impair the central vision, the development of CNV along the foveal margin of patchy atrophy impairs the central vision significantly (Fig. 17.14) [81]. The CNV develops especially in eyes with P(Lc), probably because lacquer cracks tend to develop near the fovea and thus the P(Lc) occurs in the vicinity of the central fovea. Also, different from P(D) which develops within the area of advanced diffuse atrophy with a loss of most of the choroidal thickness, P(Lc) tends to develop in the eyes with less degree of choroidal atrophy. Once the CNV develops along the edge of patchy atrophy, the chorioretinal atrophy enlarges around the CNV and fuses with P(Lc), and the posterior fundus is eventually replaced by a large area of patchy atrophy (Fig. 17.14).

### Differential Diagnosis

- *The atrophic phase of myopic CNV*

A well-defined chorioretinal atrophy develops around the scarred CNV and enlarges gradually (Fig. 17.15; see Chap. 19 for details), and the atrophic stage of myopic CNV is important to differentiate from patchy atrophy. Fundus features, angiographic findings, FAF findings, and OCT findings are all the same between the atrophic stage of myopic CNV and patchy atrophy. Especially long after the regression of myopic CNV, it becomes difficult to detect fibrovascular tissue remnants within the chorioretinal atrophy. The main difference between patchy atrophy and atrophic stage of myopic CNV is its location relative to the central fovea. The chorioretinal atrophy around the myopic CNV is almost always centered on the fovea and enlarges circumferentially around the fovea. In contrary, the patchy atrophy usually does not involve the fovea.

- *Multifocal Choroiditis (MFC) or Punctate Inner Choroidopathy (PIC)*

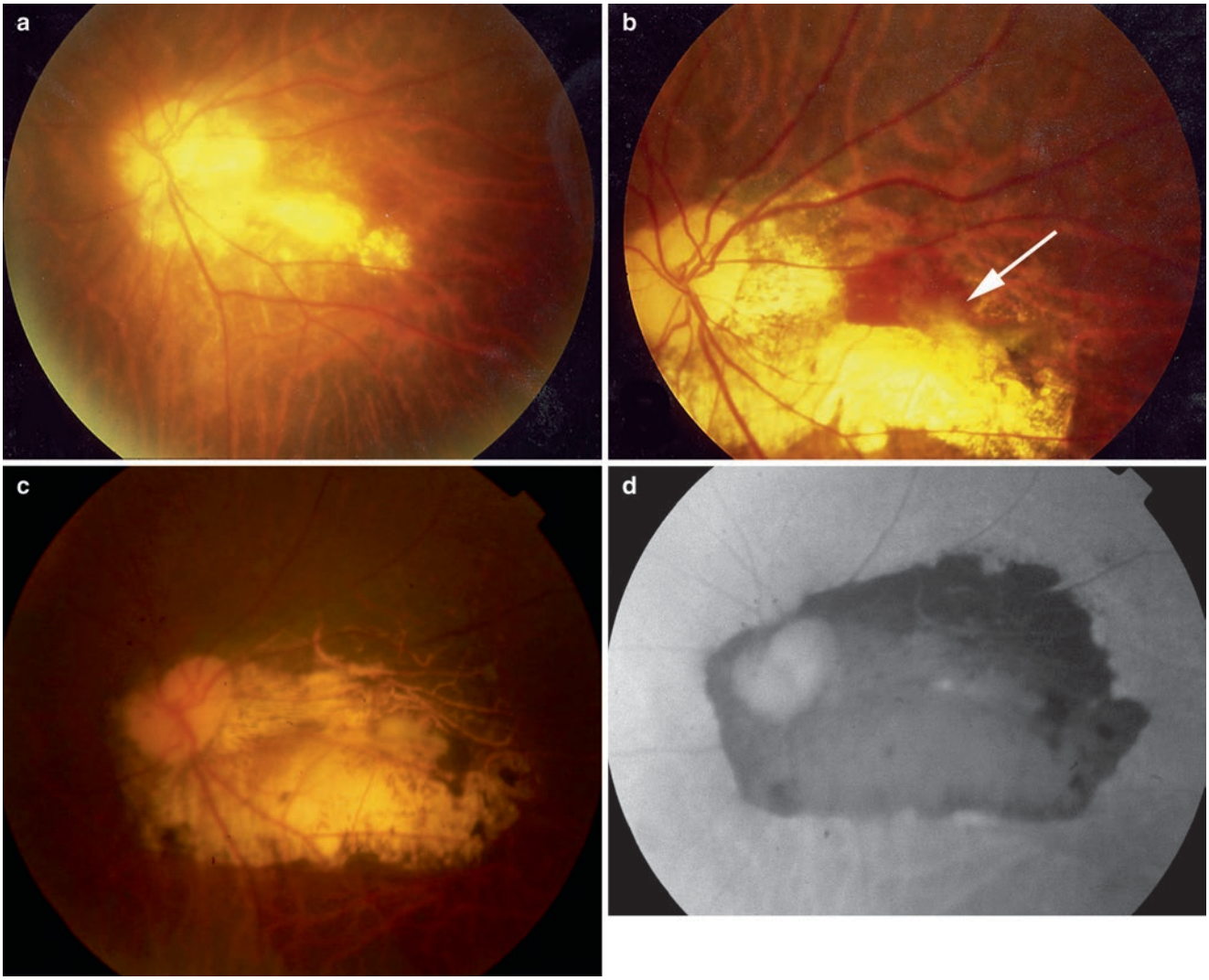


**Fig. 17.14** A fusion with P(Lc) and an atrophy around the myopic choroidal neovascularization (CNV). (**a**) At the initial visit, horizontally longitudinal P(Lc) is observed lower to the central fovea. (**b**) Two years later, the CNV has developed along the foveal edge of an enlarged P(Lc). (**c**) Ten years after the CNV regression, an atrophy developed around the scarred CNV has enlarged and fused with P(Lc). (**d**) Fundus autofluorescence shows a large area of hypo-autofluorescence in the posterior fundus

MFC and PIC tend to affect young females (~75%) who are often myopic. These patients develop focal areas of inflammation in the deep retina and choroid that progress into atrophic and pigmentary chorioretinal scars. The acute lesions are typically multiple, bilateral, and yellow-white or grayish in appearance. When we observe the lesions similar to patchy atrophy in highly myopic eyes without diffuse chorioretinal atrophy (especially in young female), we need to consider the possibility of MFC/PIC.

MFC and PIC often develop CNV; thus, the differential diagnosis is necessary between myopic CNV and CNV caused by MFC/PIC.

## 17.2.5 Others

### 17.2.5.1 Macular Lesions in Dome-Shaped Macula

Dome-shaped macula (DSM) was originally described by Gaucher and associates [82] as a convex protrusion of macula within a staphyloma in highly myopic patients. By using enhanced depth imaging OCT (EDI-OCT), Imamura and Spaide [83] showed that a DSM is a result of a relative localized thickness variation of the sclera under the macula in highly myopic patients. OCT examination is indispensable for the diagnosis of DSM. DSM is not always


**Fig. 17.15** Atrophic stage of myopic choroidal neovascularization (CNV). (**a**) Ten years after the onset of myopic CNV. Fibrovascular scar tissue is observed within the atrophy (arrow). (**b**) Eleven years after the onset of myopic CNV in an albino patient. Well-demarcated atrophy is observed around the scarred CNV. Atrophy is fused with myopic conus. (**c**) Twenty years after the onset of myopic CNV. The enlarged atrophy around the CNV is fused with P(St) as well as myopic conus

visible in all OCT scans, and it can be classified into three morphologic patterns, round dome and horizontally or vertically oval-shaped domes [84]. According to the following expanded definition, DSM can be diagnosed quantitatively as macular bulge height of >50 μm in the most convex scan in either vertical or horizontal scan [85]. The prevalence of serous RD is markedly variable from 2% to 67% depending on the series which is very rare in Asian [85–87] and much higher in Europe [82, 88]. As a mechanism of serous RD without CNV in eyes with DSM, Imamura and Spaide [83] suggested the possible obstruction of outflow of choroidal fluid by a thick sclera. Ellabban and associates [89] reported that CNV was frequently observed in eyes with DSM, in 41.2%. Gaucher et al. [82] also reported that 10 out of 15 eyes with DSM had a history of CNV. Although extrafoveal schisis was found in 17.6%, foveal schisis was uncommon in eyes with DSM, suggesting that the DSM might work in a protective fashion against the development of foveal schisis.

It is difficult to suspect the DSM solely from ophthalmoscopic findings; however, macular pigmentation and horizontal ridges connecting the optic disc and the fovea are often found in eyes with DSM and especially in the eyes whose DSM is evident only along the vertical section across the fovea [89]. Also, in the eyes with DSM along the vertical section across the fovea, the optic disc tends to be horizon-

tally long oval. Because most of the myopic disc shows vertical or vertically oblique tilting except TDS, the horizontally long oval disc appearance might provide a clue to suspect the presence of DSM.

It is noted that DSM also can be detected in 9% of highly myopic children and young adults [90]. Compared with DSM in elderly patients, the domes in children are detected only in the vertical OCT scans and have a wider basis and smoother slope of the elevation without presence of macular Bruch's membrane defect and any type of staphyloma.

### 17.2.6 Macular Lesions Along the Edge of Tilted Disc Syndrome

Macular lesions observed in eyes with DSM appear somewhat similar to the lesions observed along the upper edge of staphyloma in eyes with tilted disc syndrome (TDS), such as serous RD due to subretinal leakage [91] or CNV [92]. Maruko and Iida [93] reported that serous RD was found in 7 of 24 eyes (29%) with TDS. By using EDI-OCT and swept-source OCT, they [93] also showed that the subfoveal choroid was relatively thin and the subfoveal sclera thickened in TDS with a staphyloma edge at the macula. From these findings, they suggested that the characteristic anatomic subfoveal scleral alterations might lead to a thinner choroid and inhibit chorioscleral outflow. Nakanishi and associates [92] reported that macular complications were found on the upper border of inferior staphyloma in 25 of the 32 eyes (78%) with TDSMyopic maculopathy. Macular complications included the polypoidal choroidal vasculopathy (PCV) in 22%, classic CNV in 3%, focal serous RD without PCV or CNV in 41%, and RPE atrophy in 13%. It is interesting to consider the similarities between DSM and TDS.

## 17.3 Frequency of Myopic Maculopathy

In the Blue Mountains Eye Study (BMES) [61], myopic retinopathy was defined to include the following specific signs: staphyloma, lacquer cracks, Fuchs spot, and myopic chorioretinal thinning or atrophy. Based on this definition, signs of myopic retinopathy were found in 1.2% of the eligible residents aged ≥ 49 years ($n$ = 3654) who attended the BMES; staphyloma in 26 participants (0.7%), lacquer cracks in 8 participants (0.2%), Fuchs spot in 3 (0.1%), and chorioretinal atrophy in 7 (0.2%).

Using Tokoro's classification, Chen et al. [94] reported that myopic maculopathy was found in 443 of 604 eyes (73%) with high myopia (refractive error δ −6.0 D). Lacquer cracks were found to be the most prevalent type (29.1%) followed by CNV (20.7%), tessellated fundus (9.3%), patchy chorioretinal atrophy (5.8%), diffuse chorioretinal atrophy (4.6%), and macular atrophy (3.8%). Asakuma et al. [76] used Hayashi's classification [7] and reported that myopic maculopathy was found in 1.7% of 1969 Japanese residents aged ε 40 years in the Hisayama Study. Asakuma et al. [76] reported that diffuse atrophy, patchy atrophy, lacquer cracks, and macular atrophy were present in 1.7%, 0.4%, 0.2%, and 0.4% of the subjects. A worse visual acuity was associated with lacquer cracks, macular atrophy, and CNV, while better visual acuity was associated with tessellated fundus and diffuse atrophy [19]. The use of inconsistent definitions of myopic maculopathy has led to limited comparability. The META-PM classification is now consistently used by many studies for investigation of the prevalence of myopic maculopathy [95–98].

From a population-based Singapore Epidemiology of Eye Diseases (SEED) study [96] including 8716 phakic adult ≥ aged 40 years, the age-standardized prevalence of myopic maculopathy (defined as Meta-PM category 2, 3, 4, or any "plus" lesion) was 3.8% in all and varied in races, i.e., 2.3% in Indians, 3.7% in Malays, and 4.6% in Chinese. The risk of myopic maculopathy is present not only in high myopia (−8.0 D < SE ≤−5 D; 17.1%) and severe myopia (SE ≤ −8 D; 53.3%) but also in low(−3.0 D < SE ≤ 0.5 D; 7.0%) and moderate (−5.0 D < SE ≤ -3 D; 10.4%) myopia. Using the same definitions, another population-based study in Japan (the Hisayama Study) investigated the trend in the prevalence of myopic maculopathy at three time points from 1.6% in 2005, 3.0% in 2012, to 3.6% in 2017, suggesting that the prevalence of myopic maculopathy increased significantly over 12 years [97]. However, the prevalence of myopic maculopathy in rural southern China showed that the prevalence of myopic maculopathy was low as 1.4% even though staphyloma was also included into the definition of myopic maculopathy [98].

## 17.4 Progression of Myopic Maculopathy

Figure 17.16 is a scheme showing a progressive pattern of various lesions of myopic maculopathy, which is modified from the study following 806 highly myopic eyes for a mean period of 12.7 years [7]. In this study, 40.6% of the eyes showed a progression. The first sign that a highly myopic eye has progressed to the myopic maculopathy stage is the appearance of a tessellated fundus. The CNV develops from various lesions of myopic maculopathy, and the lesions eventually resulted in a formation of macular atrophy. The representative cases which showed a progression are shown in Figs. 17.17, 17.18, and 17.19. Liu et al. [20] in the Beijing Eye Study reported that at the 5-year follow-up examination, enlargement of the chorioretinal atrophy at the posterior fundus was observed in 9% of the eyes. Vongphanit et al. [61]

reported that after a mean period of 61 months, a significant progression of myopic retinopathy was observed in 17.4% (an enlargement of peripapillary atrophy and the development of patchy chorioretinal atrophy).

Based on META-PM classification, a retrospective case series study including 810 eyes of 432 highly myopic patients who had been followed for ≥10 years was conducted. After the mean follow-up of 18 years, the progression of myopic maculopathy was observed in 58.6% for all in which 74.3% in eyes with pathologic myopia at baseline. The most frequent progression patterns were an extension of peripapillary diffuse atrophy to macular diffuse atrophy in diffuse atrophy, enlargement of the original atrophic lesion in patchy atrophy, and development of patchy atrophy in lacquer cracks. From two Chinese population-based longitudinal studies, the 10-year progression rate of myopic maculopathy was 35.5% in elderly Chinese (aged 40+) (Beijing Eye study) [37], and the 5-year progression rate was also 35.3% in rural Chinese adult population (aged 30+) (Handan Eye Study) [99]. In a large highly myopic Chinese cohort (Zhongshan Ophthalmic Center-Brien Holden Vision Institute High Myopia Cohort Study), the myopic maculopathy progressed in approximately 15% of 657 highly myopic eyes over 2 years [100].

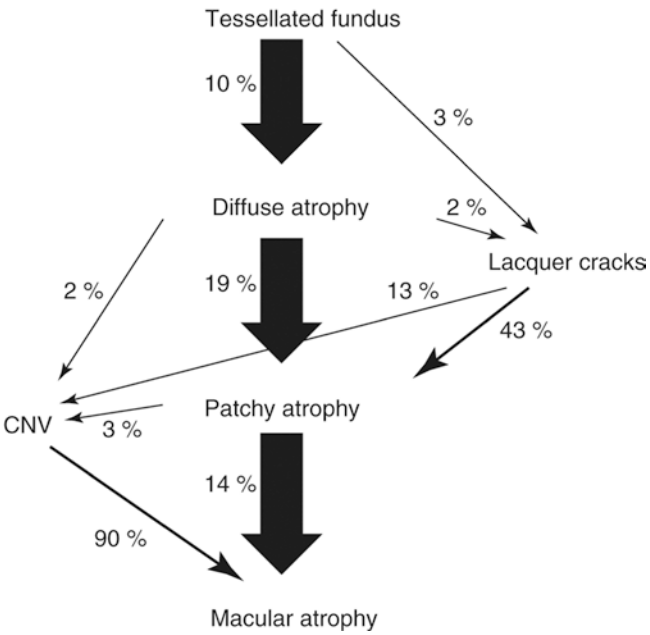


**Fig. 17.16** A scheme of progression of myopic maculopathy suggested by a long-term follow-up study (Hayashi et al. 2010). The wide arrows in the center show the most prevalent pattern of progression in highly myopic patients. The number beside the arrows indicates the rate of each progression

## 17.5 Factors Correlating with the Development of Myopic Maculopathy

Age, axial length, and posterior staphyloma are the main factors affecting the development and progression of myopic maculopathy. Higher myopic retinopathy prevalence was associated with older age [3, 42, 101]. Young patients or children tend not to develop myopic maculopathy even though the axial length is very long [21, 102, 103]. This is especially true for the atrophic lesions of myopic maculopathy, because diffuse or patchy chorioretinal atrophy usually develops in aged patients. Lacquer cracks are exceptional, and they can develop in children [102] and young patients. Chen et al. [94] analyzed the risk factors associated with myopic macu-


**Fig. 17.17** Progression from tessellated fundus to diffuse chorioretinal atrophy. (**a**) Right fundus at the age of 5 years shows a tessellated fundus. Axial length is 26.8 mm. (**b**) Twenty years later, diffuse chorioretinal atrophy has developed around the optic disc. Axial length has increased to 31.4 mm

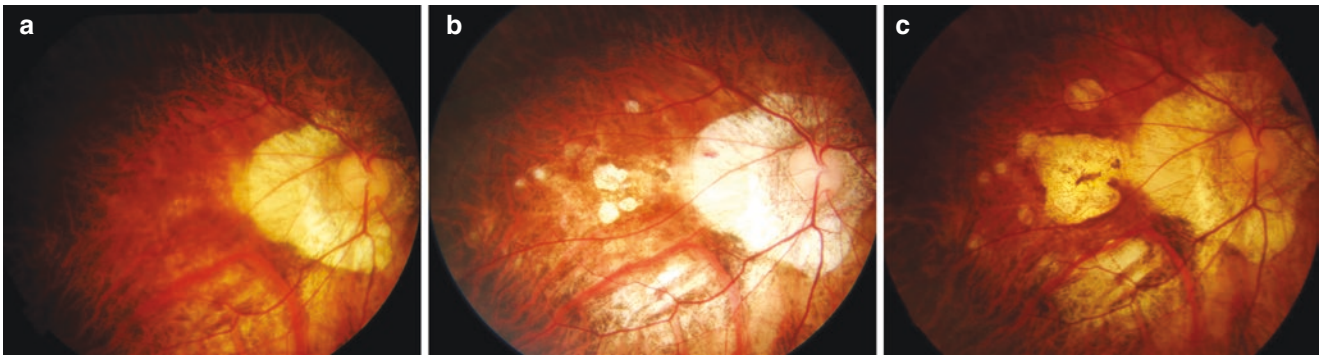


**Fig. 17.18** Progression from diffuse chorioretinal atrophy to patchy chorioretinal atrophy. (**a**) Right fundus at the age 50 years shows diffuse chorioretinal atrophy especially in the lower fundus. Axial length is 29.5 mm. (**b**) Six years later, multiple, circular lesions of patchy atrophy have developed within the area of diffuse atrophy. Axial length is 30.2 mm. (**c**) Five more years later, the lesions are enlarged and are fused with each other. Axial length is 30.6 mm

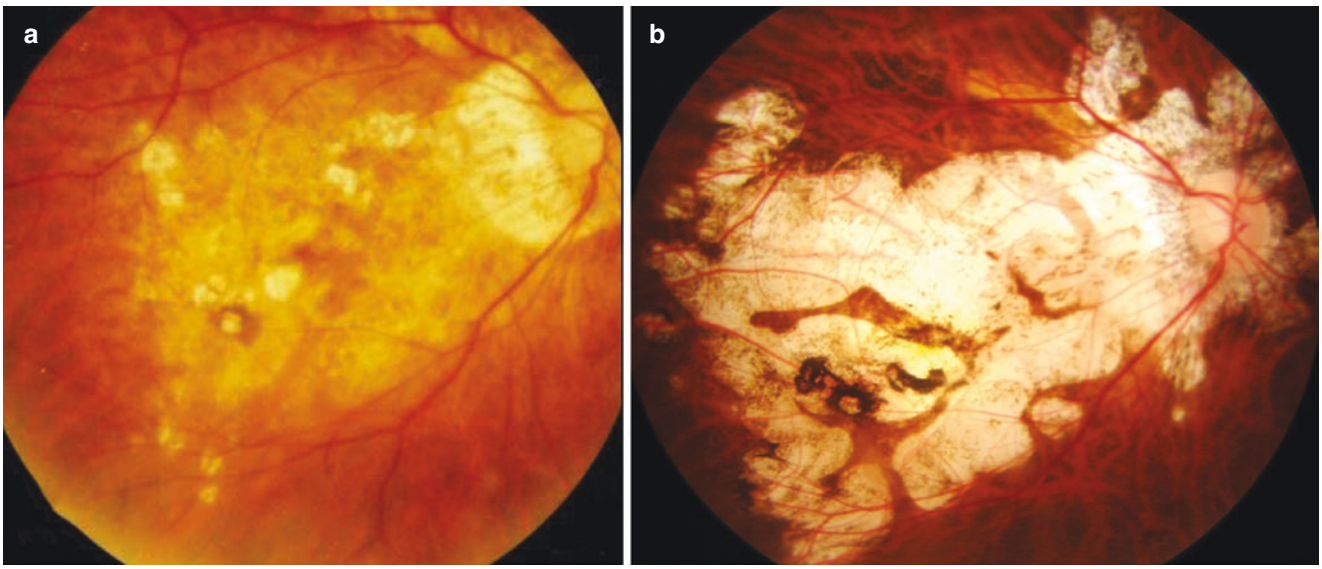


**Fig. 17.19** Enlargement and fusion of the lesions of patchy chorioretinal atrophy. (**a**) Right fundus at the age 55 years shows multiple lesions of patchy atrophy within the area of diffuse atrophy. Axial length is 30.3 mm. (**b**) Ten years later, multiple lesions of patchy atrophy are enlarged and have progressed to macular atrophy. Axial length is 31.1 mm

lopathy using general estimating equation (GEE) models. They reported that the older age was significantly associated with diffuse chorioretinal atrophy ($P = 0.024$), patchy chorioretinal atrophy ($P < 0.001$), CNV ($P < 0.001$), and macular atrophy ($P = 0.002$). Younger age was associated with lacquer cracks ($P < 0.001$).

A marked and highly non-linear relationship has been reported between refraction and the prevalence of myopic maculopathy [61, 101]. The prevalence of myopic retinopathy increased significantly ($P < 0.001$) with increasing myopic refractive error, from 3.8% in eyes with a myopic refractive error of < −4.0 diopters to 89.6% in eyes with a myopic refractive error of at least −10.0 diopters [20]. Myopes less than 5D had a myopic maculopathy prevalence of 0.42% as compared to 25.3% for myopes with greater than 5 D of myopia, i.e., a 60-fold increase in risk in high myopes. A higher degree of myopia was a risk factor for almost all kinds of maculopathy, tessellated fundus, lacquer cracks, diffuse chorioretinal atrophy, patchy chorioretinal atrophy, and macular atrophy, whereas a lower degree of myopia was associated with CNV [94]. Steidl and Pruett [104, 105] reported that a linear relationship was observed between staphyloma grade and lacquer cracks and chorioretinal atrophy. However, there was an unexpected high frequency of myopic CNV in the lower staphyloma categories.

Regarding axial length, Curtin [3, 42] reported that myopic chorioretinal degeneration was found in more than 60% of the eyes whose axial length is ε 29.5 mm, whereas it was found in less than 40% in the eyes whose axial length is <29.5 mm. Lai et al. [106] reported that the eyes with axial

length of ε29 mm were more likely to have posterior pole chorioretinal lesion including chorioretinal atrophy and lacquer cracks compared with eyes with axial length of <29 mm [106].

Age and the axial length affect the development of myopic maculopathy in a combined fashion. Lai et al. [106] reported that the eyes with myopic maculopathy had significantly older age (45.0 vs 34.8 years), longer axial length (28.84 vs 26.59 mm), and higher degree of mean spherical equivalent refractive error (−16.8 vs −9.4 D) ($P < 0.001$ for all three variables).

In the study analyzing the relationship between the scleral contour and myopic chorioretinal lesions by using swept-source OCT [107], myopic fundus lesions (myopic CNV, myopic chorioretinal atrophy, and myopic traction maculopathy) were present significantly more frequently in the eyes with irregular curvature.

Reduction of retinal blood flow in highly myopic eyes measured by laser Doppler velocimetry [108] and reduced blood flow of posterior ciliary artery as well as central retinal artery measured by color Doppler ultrasonography [109] might relate to the development of myopic chorioretinal atrophy. Benavente-Perez et al. [110] reported that the compromised pulsatile and hemodynamics of central retinal artery observed in young healthy myopes are an early feature of the decrease in ocular blood flow reported in pathological myopia. Li et al. [111] reported that myopic retinopathy was associated with attenuation of retinal vessels.

Recent OCT examinations (EDI-OCT and swept-source OCT) showed that the choroid remarkably thins in highly myopic eyes different from the retinal thickness [112–114]. Nishida and Spaide [115] reported that the subfoveal choroidal thickness was inversely correlated with logarithm of the minimum angle of resolution visual acuity. Actually, the only significant predictor in the pooled data for logarithm of the minimum angle of resolution visual acuity was subfoveal choroidal thickness ($P \leq 0.001$). Wang et al. [22] reported that the BCVA correlated significantly with macular choroidal thickness in the highly myopic patients with diffuse chorioretinal atrophy. Multiple linear regression analysis showed that age and macular choroidal thickness were the variables that associated most strongly with BCVA in the patients with diffuse atrophy, whereas neither refractive error nor axial length was a significant predictor of BCVA. However, Fujiwara et al. [112] showed that there were no correlations between logMAR visual acuity and subfoveal choroidal thickness in eyes without CNV and surgery. Pang et al. [116] also found that 70% of highly myopic eyes with extremely thin choroid (mean choroidal thickness, 14 μm) still had good BCVA (20/40 or better).

Also, the decrease of neurotrophic factor, pigment epithelium-derived factor (PEDF), in the aqueous humor has been reported in highly myopic eyes [117, 118]. However, it is not certain if this is a result due to degenerative changes of RPE cells, which is a main cell producing PEDF, or due to a dilation of PEDF because of a big volume of myopic eye, or a cause of developing myopic chorioretinal atrophy.

Myopic retinopathy was not associated significantly ($P > 0.20$) with body height and weight, gender, rural versus urban region of residence, level of education, intraocular pressure, or central corneal thickness [20]. Chen et al. [19] reported a relationship between myopic maculopathy and higher systolic blood pressure after adjustment for age, sex, smoking, body mass index, diastolic blood pressure, educational levels, alcohol drinking, and histories of diabetes or taking anti-hypertension medication.

## 17.6 Future Perspective

Mainly due to a recent advance of imaging technique, much has been clarified about the characteristics of each lesion of myopic maculopathy. However, the main concern would be that the classification and definition of myopic maculopathy have not been standardized worldwide. Also, the fundus color is largely affected by the original degree of pigmentation among races. The difference between tessellated fundus and diffuse atrophy might be due to a difference in how much choroid remains. In that case, the classification based on OCT findings might become an important and powerful tool.

## References

1. Salzmann M. The choroidal changes in high myopia. Arch Ophthalmol. 1902;31:41–2.
2. Salzmann M. Die Atrophie der Aderhaut im kurzsichtigen Auge. Albrecht von Graefes Archiv fur Ophthalmologie. 1902;54:384.
3. Curtin BJ. Basic science and clinical management. In: Curtin BJ, editor. The myopias. New York: Harper and Row; 1985. p. 177.
4. Grossniklaus HE, Green WR. Pathologic findings in pathologic myopia. Retina (Philadelphia, Pa). 1992;12:127–33.
5. Avila MP, Weiter JJ, Jalkh AE, Trempe CL, Pruett RC, Schepens CL. Natural history of choroidal neovascularization in degenerative myopia. Ophthalmology. 1984;91:1573–81.
6. Tokoro T, editor. Atlas of posterior fundus changes in pathologic myopia. Tokyo: Springer-Verlag; 1998. p. 5–22.
7. Hayashi K, Ohno-Matsui K, Shimada N, et al. Long-term pattern of progression of myopic maculopathy: a natural history study. Ophthalmology. 2010;117:1595-611–1611 e1-4.
8. Iwase A, Araie M, Tomidokoro A, et al. Prevalence and causes of low vision and blindness in a Japanese adult population: the Tajimi Study. Ophthalmology. 2006;113:1354–62.
9. Huang S, Zheng Y, Foster PJ, Huang W, He M. Prevalence and causes of visual impairment in Chinese adults in urban southern China. Arch Ophthalmol. 2009;127:1362–7.
10. Zheng Y, Lavanya R, Wu R, et al. Prevalence and causes of visual impairment and blindness in an urban Indian population: the Singapore Indian Eye Study. Ophthalmology. 2011;118:1798–804.
11. Iwano M, Nomura H, Ando F, Niino N, Miyake Y, Shimokata H. Visual acuity in a community-dwelling Japanese population

and factors associated with visual impairment. Jpn J Ophthalmol. 2004;48:37–43.
12. Cotter SA, Varma R, Ying-Lai M, Azen SP, Klein R, Los Angeles Latino Eye Study G. Causes of low vision and blindness in adult Latinos: the Los Angeles Latino Eye Study. Ophthalmology. 2006;113:1574–82.
13. Buch H, Vinding T, La Cour M, Appleyard M, Jensen GB, Nielsen NV. Prevalence and causes of visual impairment and blindness among 9980 Scandinavian adults: the Copenhagen City Eye Study. Ophthalmology. 2004;111:53–61.
14. Evans JR, Fletcher AE, Wormald RP. Causes of visual impairment in people aged 75 years and older in Britain: an add-on study to the MRC trial of assessment and management of older people in the community. Br J Ophthalmol. 2004;88:365–70.
15. Kelliher C, Kenny D, O'Brien C. Trends in blind registration in the adult population of the Republic of Ireland 1996-2003. Br J Ophthalmol. 2006;90:367–71.
16. Avisar R, Friling R, Snir M, Avisar I, Weinberger D. Estimation of prevalence and incidence rates and causes of blindness in Israel, 1998-2003. Isr Med Assoc J. 2006;8:880–1.
17. Varma R, Kim JS, Burkemper BS, et al. Prevalence and causes of visual impairment and blindness in Chinese American adults: the Chinese American Eye Study. JAMA Ophthalmol. 2016;134:785–93.
18. Shih YF, Ho TC, Hsiao CK, Lin LL. Visual outcomes for high myopic patients with or without myopic maculopathy: a 10 year follow up study. Br J Ophthalmol. 2006;90:546–50.
19. Chen SJ, Cheng CY, Li AF, et al. Prevalence and associated risk factors of myopic maculopathy in elderly Chinese: the Shihpai Eye Study. Invest Ophthalmol Vis Sci. 2012;28:28.
20. Liu HH, Xu L, Wang YX, Wang S, You QS, Jonas JB. Prevalence and progression of myopic retinopathy in Chinese adults: the Beijing Eye Study. Ophthalmology. 2010;117:1763–8.
21. Kobayashi K, Ohno-Matsui K, Kojima A, et al. Fundus characteristics of high myopia in children. Jpn J Ophthalmol. 2005;49:306–11.
22. Wang NK, Lai CC, Chu HY, et al. Classification of early dry-type myopic maculopathy with macular choroidal thickness. Am J Ophthalmol. 2012;153:669-77–677 e1-2.
23. Lin T, Grimes PA, Stone RA. Expansion of the retinal pigment epithelium in experimental myopia. Vis Res. 1993;33:1881–5.
24. Harman AM, Hoskins R, Beazley LD. Experimental eye enlargement in mature animals changes the retinal pigment epithelium. Vis Neurosci. 1999;16:619–28.
25. Hosaka A. Permeability of the blood-retinal barrier in myopia. An analysis employing vitreous fluorophotometry and computer simulation. Acta Ophthalmol Suppl. 1988;185:95–9.
26. Yoshida A, Ishiko S, Kojima M, Hosaka A. Blood-ocular barrier permeability in experimental myopia. J Fr Ophtalmol. 1990;13:481–8.
27. Yoshida A, Ishiko S, Kojima M. Inward and outward permeability of the blood-retinal barrier in experimental myopia. Graefes Arch Clin Exp Ophthalmol. 1996;234:S239–42.
28. Kitaya N, Ishiko S, Abiko T, et al. Changes in blood-retinal barrier permeability in form deprivation myopia in tree shrews. Vis Res. 2000;40:2369–77.
29. Spaide RF. Age-related choroidal atrophy. Am J Ophthalmol. 2009;147:801–10.
30. Fang Y, Du R, Nagaoka N, et al. OCT-based diagnostic criteria for different stages of myopic maculopathy. Ophthalmology. 2019;126:1018–32.
31. Zhao X, Ding X, Lyu C, et al. Morphological characteristics and visual acuity of highly myopic eyes with different severities of myopic maculopathy. Retina (Philadelphia, Pa). 2018;40:461.
32. Zhou Y, Song M, Zhou M, Liu Y, Wang F, Sun X. Choroidal and retinal thickness of highly myopic eyes with early stage of myopic chorioretinopathy: tessellation. J Ophthalmol. 2018;2018:2181602.
33. Kawabata H, Adachi-Usami E. Multifocal electroretinogram in myopia. Invest Ophthalmol Vis Sci. 1997;38:2844–51.
34. Chen JC, Brown B, Schmid KL. Delayed mfERG responses in myopia. Vis Res. 2006;46:1221–9.
35. Luu CD, Lau AM, Lee SY. Multifocal electroretinogram in adults and children with myopia. Arch Ophthalmol. 2006;124:328–34.
36. Chan HL, Mohidin N. Variation of multifocal electroretinogram with axial length. Ophthalmic Physiol Opt. 2003;23:133–40.
37. Yan YN, Wang YX, Yang Y, et al. Ten-year progression of myopic maculopathy: the Beijing eye study 2001-2011. Ophthalmology. 2018;125:1253–63.
38. Fang Y, Yokoi T, Nagaoka N, et al. Progression of myopic maculopathy during 18-year follow-up. Ophthalmology. 2018;125:863–77.
39. Malagola R, Pecorella I, Teodori C, Santi G, Mannino G. Peripheral lacquer cracks as an early finding in pathological myopia. Arch Ophthalmol. 2006;124:1783–4.
40. Bottoni FG, Eggink CA, Cruysberg JR, Verbeek AM. Dominant inherited tilted disc syndrome and lacquer cracks. Eye. 1990;4:504–9.
41. Pruett RC, Weiter JJ, Goldstein RB. Myopic cracks, angioid streaks, and traumatic tears in Bruch's membrane. Am J Ophthalmol. 1987;103:537–43.
42. Curtin BJ, Karlin DB. Axial length measurements and fundus changes of the myopic eye. I. The posterior fundus. Trans Am Ophthalmol Soc. 1970;68:312–34.
43. Klein RM, Curtin BJ. Lacquer crack lesions in pathologic myopia. Am J Ophthalmol. 1975;79:386–92.
44. Brancato R, Trabucchi G, Introini U, Avanza P, Pece A. Indocyanine green angiography (ICGA) in pathological myopia. Eur J Ophthalmol. 1996;6:39–43.
45. Quaranta M, Arnold J, Coscas G, et al. Indocyanine green angiographic features of pathologic myopia. Am J Ophthalmol. 1996;122:663–71.
46. Ohno-Matsui K, Morishima N, Ito M, Tokoro T. Indocyanine green angiographic findings of lacquer cracks in pathologic myopia. Jpn J Ophthalmol. 1998;42:293–9.
47. Ikuno Y, Sayanagi K, Soga K, et al. Lacquer crack formation and choroidal neovascularization in pathologic myopia. Retina. 2008;28:1124–31.
48. Kim YM, Yoon JU, Koh HJ. The analysis of lacquer crack in the assessment of myopic choroidal neovascularization. Eye. 2011;25:937–46.
49. Wang NK, Lai CC, Chou CL, et al. Choroidal thickness and biometric markers for the screening of lacquer cracks in patients with high myopia. PLoS One. 2013;8:22.
50. Klein RM, Green S. The development of lacquer cracks in pathologic myopia. Am J Ophthalmol. 1988;106:282–5.
51. Ohno-Matsui K, Ito M, Tokoro T. Subretinal bleeding without choroidal neovascularization in pathologic myopia. A sign of new lacquer crack formation. Retina. 1996;16:196–202.
52. Yip LW, Au Eong KG. Recurrent subretinal haemorrhages and progressive lacquer cracks in a high myope. Acta Ophthalmol Scand. 2003;81:646–7.
53. Moriyama M, Ohno-Matsui K, Shimada N, et al. Correlation between visual prognosis and fundus autofluorescence and optical coherence tomographic findings in highly myopic eyes with submacular hemorrhage and without choroidal neovascularization. Retina. 2011;31:74–80.
54. Hirata A, Negi A. Lacquer crack lesions in experimental chick myopia. Graefes Arch Clin Exp Ophthalmol. 1998;236:138–45.
55. Ellies P, Pietrini D, Lumbroso L, Lebuisson DA. Macular hemorrhage after laser in situ keratomileusis for high myopia. J Cataract Refract Surg. 2000;26:922–4.

56. Loewenstein A, Lipshitz I, Varssano D, Lazar M. Macular hemorrhage after excimer laser photorefractive keratectomy. J Cataract Refract Surg. 1997;23:808–10.
57. Luna JD, Reviglio VE, Juarez CP. Bilateral macular hemorrhage after laser in situ keratomileusis. Graefes Arch Clin Exp Ophthalmol. 1999;237:611–3.
58. Principe AH, Lin DY, Small KW, Aldave AJ. Macular hemorrhage after laser in situ keratomileusis (LASIK) with femtosecond laser flap creation. Am J Ophthalmol. 2004;138:657–9.
59. Loewenstein A, Goldstein M, Lazar M. Retinal pathology occurring after excimer laser surgery or phakic intraocular lens implantation: evaluation of possible relationship. Surv Ophthalmol. 2002;47:125–35.
60. Johnson DA, Yannuzzi LA, Shakin JL, Lightman DA. Lacquer cracks following laser treatment of choroidal neovascularization in pathologic myopia. Retina. 1998;18:118–24.
61. Vongphanit J, Mitchell P, Wang JJ. Prevalence and progression of myopic retinopathy in an older population. Ophthalmology. 2002;109:704–11.
62. Ohno-Matsui K, Tokoro T. The progression of lacquer cracks in pathologic myopia. Retina (Philadelphia, Pa). 1996;16:29–37.
63. Xu X, Fang Y, Uramoto K, et al. Clinical features of Lacquer Cracks in eyes with pathologic myopia. Retina (Philadelphia, Pa). 2019;39:1265–77.
64. Yannuzzi LA. The retinal atlas. New York: Elsevier; 2010. p. 526–43.
65. Shinohara K, Moriyama M, Shimada N, Tanaka Y, Ohno-Matsui K. Myopic stretch lines: linear lesions in fundus of eyes with pathologic myopia that differ from lacquer cracks. Retina. 2014;34(3):461–9.
66. Freund KB, Ciardella AP, Yannuzzi LA, et al. Peripapillary detachment in pathologic myopia. Arch Ophthalmol. 2003;121:197–204.
67. Freund KB, Mukkamala SK, Cooney MJ. Peripapillary choroidal thickening and cavitation. Arch Ophthalmol. 2011;129:1096–7.
68. Shimada N, Ohno-Matsui K, Yoshida T, et al. Characteristics of peripapillary detachment in pathologic myopia. Arch Ophthalmol. 2006;124:46–52.
69. Spaide RF, Akiba M, Ohno-Matsui K. Evaluation of peripapillary intrachoroidal cavitation with swept source and enhanced depth imaging optical coherence tomography. Retina. 2012;32:1037–44.
70. Toranzo J, Cohen SY, Erginay A, Gaudric A. Peripapillary intrachoroidal cavitation in myopia. Am J Ophthalmol. 2005;140:731–2.
71. Shin JY, Yu HG. Visual prognosis and spectral-domain optical coherence tomography findings of myopic foveoschisis surgery using 25-gauge transconjunctival sutureless vitrectomy. Retina. 2012;32:486–92.
72. Ohno-Matsui K, Jonas JB, Spaide RF. Macular Bruch membrane holes in highly myopic patchy chorioretinal atrophy. Am J Ophthalmol. 2016;166:22–8.
73. Du R, Fang Y, Jonas JB, et al. Clinical features of patchy chorioretinal atrophy in pathologic myopia. Retina (Philadelphia, Pa). 2019;40:951.
74. Jonas JB, Ohno-Matsui K, Spaide RF, Holbach L, Panda-Jonas S. Macular Bruch's membrane defects and axial length: association with gamma zone and delta zone in peripapillary region. Invest Ophthalmol Vis Sci. 2013;54:1295–302.
75. Ohno-Matsui K, Akiba M, Moriyama M, Ishibashi T, Hirakata A, Tokoro T. Intrachoroidal cavitation in macular area of eyes with pathologic myopia. Am J Ophthalmol. 2012;154:382–93.
76. Asakuma T, Yasuda M, Ninomiya T, et al. Prevalence and risk factors for myopic retinopathy in a Japanese population: the Hisayama Study. Ophthalmology. 2012;10:10.
77. Ito-Ohara M, Seko Y, Morita H, Imagawa N, Tokoro T. Clinical course of newly developed or progressive patchy chorioretinal atrophy in pathological myopia. Ophthalmologica. 1998;212:23–9.
78. Baba T, Ohno-Matsui K, Futagami S, et al. Prevalence and characteristics of foveal retinal detachment without macular hole in high myopia. Am J Ophthalmol. 2003;135:338–42.
79. Fang X, Zheng X, Weng Y, et al. Anatomical and visual outcome after vitrectomy with triamcinolone acedonide-assisted epiretinal membrane removal in highly myopic eyes with retinal detachment due to macular hole. Eye. 2009;23:248–54.
80. Chen L, Wang K, Esmaili DD, Xu G. Rhegmatogenous retinal detachment due to paravascular linear retinal breaks over patchy chorioretinal atrophy in pathologic myopia. Arch Ophthalmol. 2010;128:1551–4.
81. Ohno-Matsui K, Yoshida T, Futagami S, et al. Patchy atrophy and lacquer cracks predispose to the development of choroidal neovascularisation in pathological myopia. Br J Ophthalmol. 2003;87:570–3.
82. Gaucher D, Erginay A, Lecleire-Collet A, et al. Dome-shaped macula in eyes with myopic posterior staphyloma. Am J Ophthalmol. 2008;145:909–14.
83. Imamura Y, Iida T, Maruko I, Zweifel SA, Spaide RF. Enhanced depth imaging optical coherence tomography of the sclera in dome-shaped macula. Am J Ophthalmol. 2011;151:297–302.
84. Caillaux V, Gaucher D, Gualino V, Massin P, Tadayoni R, Gaudric A. Morphologic characterization of dome-shaped macula in myopic eyes with serous macular detachment. Am J Ophthalmol. 2013;156:958–967.e1.
85. Ellabban AA, Tsujikawa A, Matsumoto A, et al. Three-dimensional tomographic features of dome-shaped macula by swept-source optical coherence tomography. Am J Ophthalmol. 2013;155:320–328 e2.
86. Liang IC, Shimada N, Tanaka Y, et al. Comparison of clinical features in highly myopic eyes with and without a dome-shaped macula. Ophthalmology. 2015;122:1591–600.
87. Zhao X, Ding X, Lyu C, et al. Observational study of clinical characteristics of dome-shaped macula in Chinese Han with high myopia at Zhongshan Ophthalmic Centre. BMJ Open. 2018;8:e021887.
88. Viola F, Dell'Arti L, Benatti E, et al. Choroidal findings in dome-shaped macula in highly myopic eyes: a longitudinal study. Am J Ophthalmol. 2015;159:44–52.
89. Ellabban AA, Tsujikawa A, Matsumoto A, et al. Three-dimensional tomographic features of dome-shaped macula by swept-source optical coherence tomography. Am J Ophthalmol. 2012;3:00578.
90. Xu X, Fang Y, Jonas JB, et al. Ridge-shaped macula in young myopic patients and its differentiation from typical dome-shaped macula in elderly myopic patients. Retina (Philadelphia, Pa). 2018;40:225.
91. Cohen SY, Quentel G, Guiberteau B, Delahaye-Mazza C, Gaudric A. Macular serous retinal detachment caused by subretinal leakage in tilted disc syndrome. Ophthalmology. 1998;105:1831–4.
92. Nakanishi H, Tsujikawa A, Gotoh N, et al. Macular complications on the border of an inferior staphyloma associated with tilted disc syndrome. Retina. 2008;28:1493–501.
93. Maruko I, Iida T, Sugano Y, Oyamada H, Sekiryu T. Morphologic choroidal and scleral changes at the macula in tilted disc syndrome with staphyloma using optical coherence tomography. Invest Ophthalmol Vis Sci. 2011;52:8763–8.
94. Chen H, Wen F, Li H, et al. The types and severity of high myopic maculopathy in Chinese patients. Ophthalmic Physiol Opt. 2012;32:60–7.
95. Choudhury F, Meuer SM, Klein R, et al. Prevalence and characteristics of myopic degeneration in an adult Chinese American population: the Chinese American Eye Study. Am J Ophthalmol. 2018;187:34–42.
96. Wong YL, Sabanayagam C, Ding Y, et al. Prevalence, risk factors, and impact of myopic macular degeneration on visual impairment

and functioning among adults in Singapore. Invest Ophthalmol Vis Sci. 2018;59:4603–13.
97. Ueda E, Yasuda M, Fujiwara K, et al. Trends in the prevalence of myopia and myopic maculopathy in a Japanese population: the Hisayama Study. Invest Ophthalmol Vis Sci. 2019;60:2781–6.
98. Li Z, Liu R, Jin G, et al. Prevalence and risk factors of myopic maculopathy in rural southern China: the Yangxi Eye Study. Br J Ophthalmol. 2019;103:1797.
99. Lin C, Li SM, Ohno-Matsui K, et al. Five-year incidence and progression of myopic maculopathy in a rural Chinese adult population: the Handan Eye Study. Ophthalmic Physiol Opt. 2018;38:337–45.
100. Li Z, Liu R, Xiao O, et al. Progression of myopic maculopathy in highly myopic Chinese eyes. Invest Ophthalmol Vis Sci. 2019;60:1096–104.
101. Gao LQ, Liu W, Liang YB, et al. Prevalence and characteristics of myopic retinopathy in a rural Chinese adult population: the Handan Eye Study. Arch Ophthalmol. 2011;129:1199–204.
102. Samarawickrama C, Mitchell P, Tong L, et al. Myopia-related optic disc and retinal changes in adolescent children from Singapore. Ophthalmology. 2011;118:2050–7.
103. Tong L, Saw SM, Chua WH, et al. Optic disk and retinal characteristics in myopic children. Am J Ophthalmol. 2004;138:160–2.
104. Steidl SM, Pruett RC. Macular complications associated with posterior staphyloma. Am J Ophthalmol. 1997;123:181–7.
105. Pruett RC. Complications associated with posterior staphyloma. Curr Opin Ophthalmol. 1998;9:16–22.
106. Lai TY, Fan DS, Lai WW, Lam DS. Peripheral and posterior pole retinal lesions in association with high myopia: a cross-sectional community-based study in Hong Kong. Eye. 2008;22:209–13.
107. Ohno-Matsui K, Akiba M, Modegi T, et al. Association between shape of sclera and myopic retinochoroidal lesions in patients with pathologic myopia. Invest Ophthalmol Vis Sci. 2012;9:9.
108. Shimada N, Ohno-Matsui K, Harino S, et al. Reduction of retinal blood flow in high myopia. Graefes Arch Clin Exp Ophthalmol. 2004;242:284–8.
109. Akyol N, Kukner AS, Ozdemir T, Esmerligil S. Choroidal and retinal blood flow changes in degenerative myopia. Can J Ophthalmol. 1996;31:113–9.
110. Benavente-Perez A, Hosking SL, Logan NS, Broadway DC. Ocular blood flow measurements in healthy human myopic eyes. Graefes Arch Clin Exp Ophthalmol. 2010;248:1587–94.
111. Li H, Mitchell P, Rochtchina E, Burlutsky G, Wong TY, Wang JJ. Retinal vessel caliber and myopic retinopathy: the Blue Mountains Eye Study. Ophthalmic Epidemiol. 2011;18:275–80.
112. Fujiwara T, Imamura Y, Margolis R, Slakter JS, Spaide RF. Enhanced depth imaging optical coherence tomography of the choroid in highly myopic eyes. Am J Ophthalmol. 2009;148:445–50.
113. Ikuno Y, Tano Y. Retinal and choroidal biometry in highly myopic eyes with spectral-domain optical coherence tomography. Invest Ophthalmol Vis Sci. 2009;50:3876–80.
114. Barteselli G, Chhablani J, El-Emam S, et al. Choroidal volume variations with age, axial length, and sex in healthy subjects: a three-dimensional analysis. Ophthalmology. 2012;119:2572–8.
115. Nishida Y, Fujiwara T, Imamura Y, Lima LH, Kurosaka D, Spaide RF. Choroidal thickness and visual acuity in highly myopic eyes. Retina (Philadelphia, Pa). 2012;32:1229–36.
116. Pang CE, Sarraf D, Freund KB. Extreme choroidal thinning in high myopia. Retina (Philadelphia, Pa). 2015;35:407-15.
117. Ogata N, Imaizumi M, Miyashiro M, et al. Low levels of pigment epithelium-derived factor in highly myopic eyes with chorioretinal atrophy. Am J Ophthalmol. 2005;140:937–9.
118. Shin YJ, Nam WH, Park SE, Kim JH, Kim HK. Aqueous humor concentrations of vascular endothelial growth factor and pigment epithelium-derived factor in high myopic patients. Mol Vis. 2012;18:2265–70.